

1 **Analogue experiments on releasing and restraining bends and their**  
2 **application to the study of the Barents Shear Margin**

3  
4  
5  
6 **Roy H. Gabrielsen** <sup>1)</sup>, **Panagiotis A. Giannenas**<sup>x)</sup>, **Dimitrios Sokoutis**<sup>1,3)</sup>, **Ernst**  
7 **Willingshofer**<sup>3)</sup>, **Muhammad Hassaan**<sup>1,4)</sup> & **Jan Inge Faleide**<sup>1)</sup>

8  
9 <sup>1)</sup>Department of Geosciences, University of Oslo, Norway

10 <sup>2)</sup>panagiotis-athanasios.giannenos@univ-rennes1.fr

11 <sup>3)</sup> Faculty of Geosciences, Utrecht University, the Netherlands

12 <sup>4)</sup> Vår Energi AS, Grundingen 3, 0250 Oslo, Norway

13  
14  
15 **Corresponding author: Roy H. Gabrielsen** ([r.h.gabrielsen@geo.uio.no](mailto:r.h.gabrielsen@geo.uio.no))

16  
17 **ORCI-id:**

18 Jan Inge Faleide: 0000-0001-8032-2015

19 Roy H. Gabrielsen: 0000-0001-5427-8404

20 Muhammad Hassaan: 0000-0001-6004-8557

21  
22  
23  
24  
25 **Abstract:**

26 The Barents Shear Margin separates the Svalbard and Barents Sea from the North  
27 Atlantic. During the break-up of the North Atlantic the plate tectonic configuration  
28 was characterized by sequential dextral shear, extension, and finally contraction  
29 and inversion. This generated a complex zone of deformation that contains several  
30 structural families of over-lapping and reactivated structures.

31 A series of crustal-scale analogue experiments, utilizing a scaled stratified sand-  
32 silicon polymer sequence were utilized in the study of the structural evolution of  
33 the shear margin.

34  
35 The most significant observations of particular significance for interpreting the  
36 structural configuration of the Barents Shear Margin are:

37 1) Prominent early-stage positive structural elements (e.g. folds, push-ups)  
38 interacted with younger (e.g. inversion) structures and contributed to a hybrid  
39 final structural pattern.

40 2) Several structural features that were initiated during the early (dextral shear)  
41 stage became overprinted and obliterated in the subsequent stages.

42 3) All master faults, pull-part basins and extensional shear duplexes initiated  
43 during the shear stage quickly became linked in the extension stage, generating a  
44 connected basin system along the entire shear margin at the stage of maximum  
45 extension.

46 4) The fold pattern generated during the terminal stage (contraction/inversion  
47 became dominant in the basin areas and was characterized by fold axes striking  
48 parallel to the basin margins. These folds, however, strongly affected the shallow  
49 intra-basin layers.

50 The experiments reproduced the geometry and positions of the major basins and  
51 relations between structural elements (fault and fold systems) as observed along  
52 and adjacent to the Barents Shear Margin. This supports the present structural  
53 model for the shear margin.

54  
55

56 **Plain language summary:**

57 The Barents Shear Margin defines the border between the relatively shallow  
58 Barents Sea that is situated on a continental plate, and the deep ocean. The margin  
59 is characterized by a complex structural pattern that has resulted from the  
60 opening and separation of the continent and the ocean, starting c. 65 million years  
61 ago. This history included on phase of right-lateral shear and one phase of  
62 spreading, the latter including a sub phase of shortening, perhaps due to plate  
63 tectonic reorganizations. The area has been mapped by the study of reflection  
64 seismic lines for decades, but many details of its development is not yet fully  
65 constrained. We therefore ran a set of scaled experiments to investigate what kind  
66 of structures could be expected in this kind of tectonic environment, and to figure  
67 out what is a reasonable time relation between them. From these experiments we  
68 deduced several types of structures/faults, folds and sedimentary basins) that  
69 helps us to improve the understanding of the history of the opening of the North  
70 Atlantic.

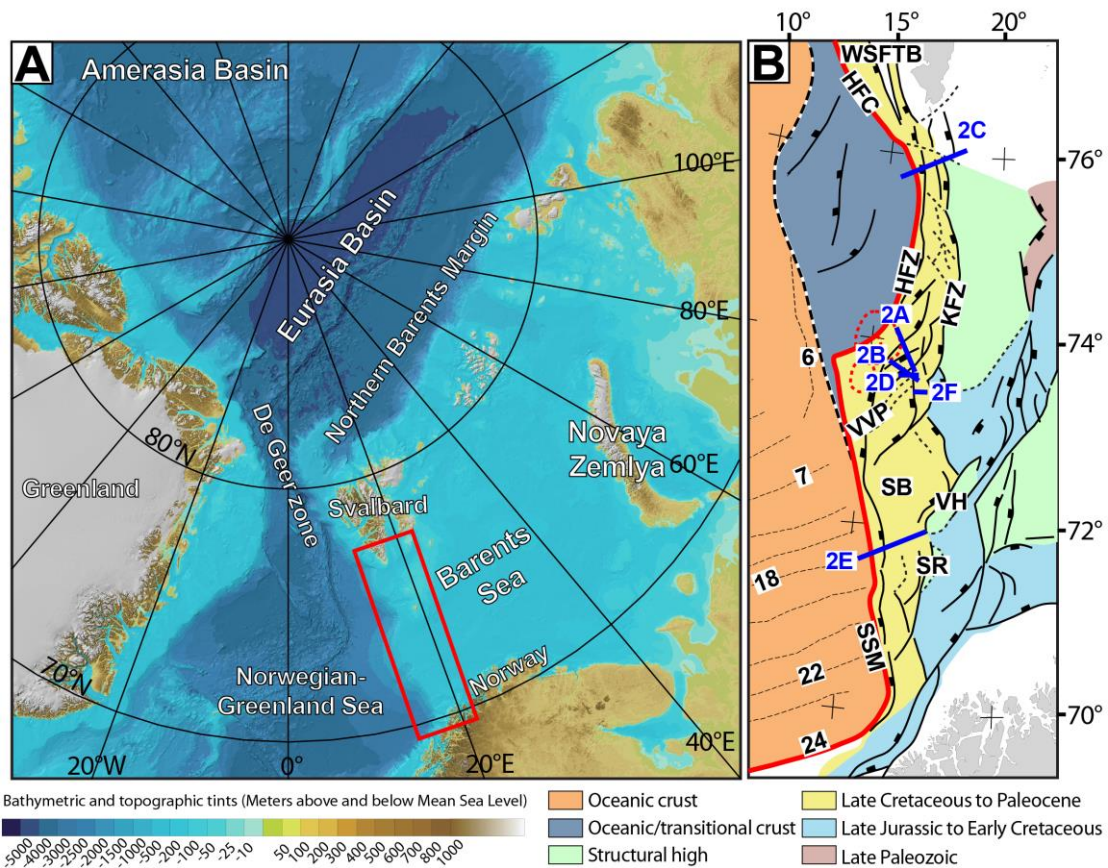
71  
72  
73

74 **Key words:** Analogue experiments, dextral strike-slip, releasing and restraining  
75 bends, multiple folding, Barents Shear Margin, basin inversion

76  
77

78 **Introduction**

79  
80 Physiography, width and structural style of the Norwegian continental margin  
81 vary considerably along its strike (e.g. Faleide et al., 2008, 2015). The margin  
82 includes a southern rifted segment between 60° and 70°N and a northern sheared-  
83 rifted segment between 70° and 82°N (**Figure 1A**). The latter coincides with the  
84 ocean-ward border of the western Barents Sea and Svalbard margins (e.g. Faleide  
85 et al., 2008) and is referred to here as “the Barents Shear Margin”. This segment  
86 coincides with the continent-ocean transition (COT) of the northernmost part of  
87 the North Atlantic Ocean, and its configuration is typical for that of transform  
88 margins where the structural pattern became established in an early stage of  
89 shear, later to develop into an active continent-ocean passive margin (Mascle &  
90 Blarez, 1987; Lorenzo, 1997; Seiler et al., 2010; Basile, 2015; Nemcok et al., 2016).  
91 Late Cretaceous - Palaeocene shear, rifting, breakup and incipient spreading in the  
92 North Atlantic was associated with voluminous magmatic activity, resulting in the  
93 development of the North Atlantic Volcanic Province (Saunders et al., 1997;  
94 Ganerød et al., 2010; Horni, 2017). According to its tectonic development, the  
95 Barents Shear Margin (**Figure 1B**) incorporates, or is bordered by, several distinct  
96 structural elements, some of which are associated with volcanism and halokinesis.  
97 The multistage development combined with a complex geometry caused  
98 interference between structures (and sediment systems) in different stages of the  
99 margin development. Such relations are not always obvious, but interpretation  
100 can be supported by the help of scale-models. Combining the interpretation of  
101 reflection seismic data and analogue modeling, therefore, we investigate  
102 structures generated in (initial) dextral shear, the development into seafloor  
103 spreading and subsequent contraction in this process, the later stages  
104 (contraction) of which were likely influenced by plate reorganization (Talwani &  
105 Eldholm, 1977, Gaina et al. 2009, see also see also Vågnes et al. 1998; Pascal &  
106 Gabrielsen 2001; Pascal et al., 2005; Gac et al., 2016) or other far-field stresses  
107 (Doré & Lundin, 1996; Lundin & Doré, 1997; Doré et al., 1999; 2016; Lundin et al.,  
108 2013). The present experiments were designed to illuminate the structural  
109 complexity affiliated with multistage sheared passive margins, so that the  
110 significance of structural elements like fault and fold systems observed along the  
111 Barents Shear Margin could be set into a dynamic context. The study area suffered



112

113 **Figure 1: A)** The Barents Sea provides is separated from the Norwegian-  
 114 Greenland Sea by the de Geer transfer margin. Red box shows the present study  
 115 area. **B)** Structural map Barents Sea shear margin. Note segmentation of the  
 116 continent-ocean transition. Abbreviations (from north to south): WSFTB = West  
 117 Spitsbergen Fold-and-Thrust Belt HFZ=Hornsund Fault Complex, KFC = Knølegga  
 118 Fault Zone, VVP = Vestbakken Volcanic Province, SB = Sørvestsnaget Basin,  
 119 VH=Veslemøy High, SR = Senja Ridge, SSM = Senja Shear Margin. Blue lines  
 120 indicate position of seismic profiles in Figure 2 and red line X-X' shows western  
 121 border of thinned crust (see also Figure 3). Chron numbers are indicated on  
 122 oceanic crust area.

123

124 repeated and contrasting stages of deformation, including dextral shear, oblique  
 125 extension, inversion and volcanic activity. This is a particular challenge in such  
 126 tectonic settings that are characterized by repeated overprinting and  
 127 canabalization of younger structural elements. The experimental approach opens  
 128 for the identification and characterization of the different stages of deformation  
 129 and their affiliated structural elements precedingthe present-day margin  
 130 geometry.

131

132

133 **Regional background**

134 In the following sections we provide definitions and a short description of the  
135 main structural elements constituting the study area. The structural elements are  
136 presented in-sequence from north to south and (**Figure 1B**).

137

138 The greater **Barents Shear Margin** is a part of the more extensive De Geer Zone  
139 megashear system which linked the Norwegian Greenland Sea and the Arctic  
140 Eurasia system (Eldholm et al., 1987; 2002; Faleide et al., 1988; Breivik et al.,  
141 1998; 2003). Together with its conjugate Greenland counterpart it carries the  
142 evidence of post-Caledonian extension that culminated with Cenozoic break-up of  
143 the North Atlantic (e.g. Brekke, 2000; Gabrielsen et al., 1990; Faleide et al., 1993;  
144 Gudlaugsson et al., 1998). Two shear margin segments are separated by a central  
145 rift-dominated segment along the Barents Shear Margin (Myhre et al., 1982;  
146 Vågnes, 1997; Myhre & Eldholm, 1988; Ryseth et al., 2003; Faleide et al., 1988;  
147 1993; 2008). Each segment maintained the structural and magmatic  
148 characteristics of the crust during its development. Of these the Senja Shear  
149 Margin is the southernmost segment, originally termed the Senja Fracture Zone  
150 by Eldholm et al., (1987). Here NNW-SSE-striking folds interfere with NE-SW-  
151 striking structures (Giannenas, 2018). Strain partitioning characterizes the of the  
152 shear zone system (e.g. Vest Spitsbergen; Leever et al. 2011a,b and the  
153 Sørvestsnaget Basin; Kristensen et al., 2017).

154

155 **The Hornsund Fault Zone and West Spitsbergen Fold-and Thrust Belt** form  
156 the northernmost segment of the Barents Shear Margin and coincide with the  
157 southern continuation of the De Geer Zone and the Senja Shear Margin. The  
158 presently distinguishable master fault of this system is the Hornsund Fault Zone,  
159 which together with the West Spitsbergen fold-and-thrust-belt provides a type  
160 setting for transpression and strain partitioning (Harland, 1965; 1969; 1971;  
161 Lowell, 1972; Gabrielsen et al., 1992; Maher et al., 1997; Leever et al., 2011 a,b).  
162 Plate tectonic reconstructions suggest that the plate boundary accommodated c.  
163 750 km along-strike dextral displacement and 20-40 km of shortening in the  
164 Eocene (Bergh et al., 1997; Gaina et al., 2009).

165

166 **The Knølegga Fault Zone** can be seen as a part of the Hornsund fault system  
167 extending from the southern tip of Spitsbergen (Gabrielsen et al., 1990). It trends  
168 NNE-SSW to N-S and defines the western margin of the Stappen High. The vertical  
169 displacement approaches 6 km. Although the main movements along the fault may  
170 be Tertiary of age, it is likely that it was initiated much earlier. The Tertiary  
171 displacement may have a lateral (dextral) component (Gabrielsen et al., 1990).

172

173 **The Vestbakken Volcanic Province** is the main topic of this contribution. It  
174 represents the central rifted segment of the Senja Shear Margin and links the  
175 sheared margin segments to the north and south occupying a right-double  
176 stepping (eastward) releasing-bend-setting. Prominent volcanoes and sill-  
177 intrusions suggest three distinct volcanic events in the Vestbakken Volcanic  
178 Province (Jebsen & Faleide, 1998; Faleide et al., 2008; Libak et al., 2012). It is  
179 constrained to its east by the eastern boundary fault (EBF in **Figure 1B**), that is a  
180 part of the Knølegga Fault Complex, separating the Vestbakken Volcanic Province  
181 from the marginal Stappen High to the east. To the south and southeast the  
182 Vestbakken Volcanic Province drops gradually towards the Sørvestsnaget Basin  
183 across the southern extension of the eastern boundary fault and its associated  
184 faults. To the west and north the area is delineated by the continent – ocean  
185 boundary/transition. The Vestbakken Volcanic Province includes both  
186 extensional and contractional structures (eg. Jebsen & Faleide, 1998; Faleide et al.,  
187 2008; Blaich et al., 2017).

188 -

189 , and Two main episodes of Cenozoic extensional faulting were identified in the  
190 Vestbakken Volcanic Province: (i) a late Paleocene-early Eocene event, which  
191 correlates in time with the continental break-up in the Norwegian-Greenland Sea,  
192 (ii) an early Oligocene event that is tentatively correlated to plate reorganization  
193 around 34 Ma activated NE-SW striking faults. Volcanic activity coincides with  
194 these events.

195

196 **The Sørvestsnaget Basin** occupies the area east the COT between 71 and 73°N  
197 and is characterized by an exceptionally thick Cretaceous-Cenozoic sequence  
198 (Gabrielsen et al., 1990). To the west it is delineated by the Senja Shear Margin

199 and to the northeast it is separated from the Bjørnøya Basin by the southern part  
200 of the Knølegga Fault Complex (Faleide et al., 1988). The position of the Senja  
201 Ridge coincides with southeastern border of the Sørvestsnaget Basin (Figure 1B),  
202 whereas the Vestbakken Volcanic Province is situated to its north. An episode of  
203 Cretaceous rifting in the Sørvestsnaget Basin climaxed in the Cenomanian-middle  
204 Turonian (Breivik et al., 1998), succeeded by Late Cretaceous-Palaeocene fast  
205 sedimentation (Ryseth et al., 2003). Particularly the later stages of the basin  
206 formation were strongly influenced by the opening of the North Atlantic (Hanisch,  
207 1984; Brekke & Riis, 1987). Salt diapirism also contributed to the development of  
208 this basin (Perez-Garcia et al., 2013).

209

210 **The Senja Ridge** (SR in **Figure 1B**) runs parallel to the continental margin and  
211 coincides with the western border of the Tromsø Basin. It is characterized by a N-  
212 S-trending gravity anomaly which are interpreted as buried mafic-ultramafic  
213 intrusions which are associated with the Seiland Igneous Province (Fichler &  
214 Pastore 2022). The structural development of the Senja Ridge has been associated  
215 with shear affiliated with the development of the shear margin (Riis et al. 1986).  
216 and though it was a positive structural element from the mid Cretaceous to the  
217 Pliocene it may have been activated at an even earlier stage (Gabrielsen et al.  
218 1990).

219

220 **The Senja Shear Margin** was active during the Eocene opening of the Norwegian-  
221 Greenland Sea dextral shear that split out slivers of continental crust. These slivers  
222 became embedded in the oceanic crust during continued seafloor spreading  
223 (Faleide et al., 2008). The Senja Shear Margin coincides with the western margin  
224 of a basin system superimposed on an area of significant crustal thinning. This  
225 part of the shear margin was characterized by a composite architecture even at  
226 the earliest stages of its development (Faleide et al., 2008). The basin system  
227 accumulated sedimentary thicknesses in places exceeding 15 km. Subsequent  
228 shearing contributed to the development of releasing and restraining bends,  
229 associated pull-apart-basins, neutral strike-slip segments, flower-structures and  
230 fold-systems (*sensu* Crowell, 1974 a,b; Biddle & Christie-Blick, 1985a,b;

231 Cunningham & Mann, 2007a,b). Particularly the hanging wall west of the Knølegga  
232 Fault Complex

233

234 (see below) of the Barents Shear Margin was affected by wrench deformation as  
235 seen from several push-ups and fold systems (Grogan et al., 1999; Bergh & Grogan  
236 2003). The structural development of the margin was complicated by active  
237 halokinesis (Knutsen & Larsen, 1997; Gudlaugsson et al., 1998; Ryseth et al.,  
238 2003).

239

240

### 241 **Reflection seismic data and structural interpretation**

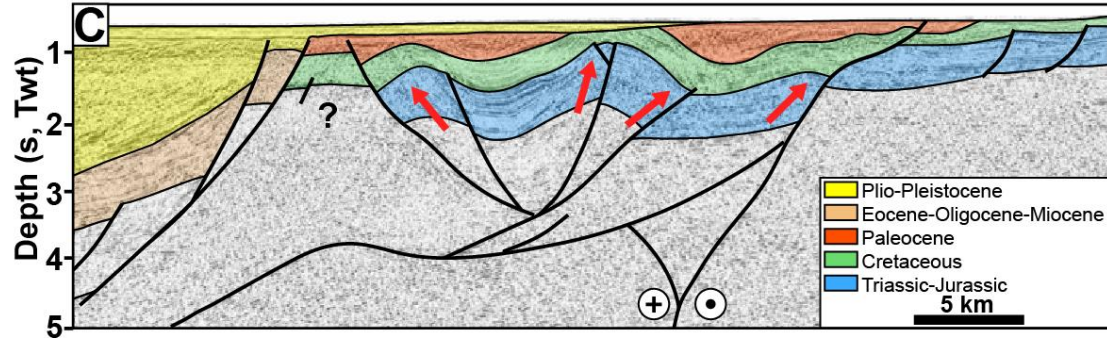
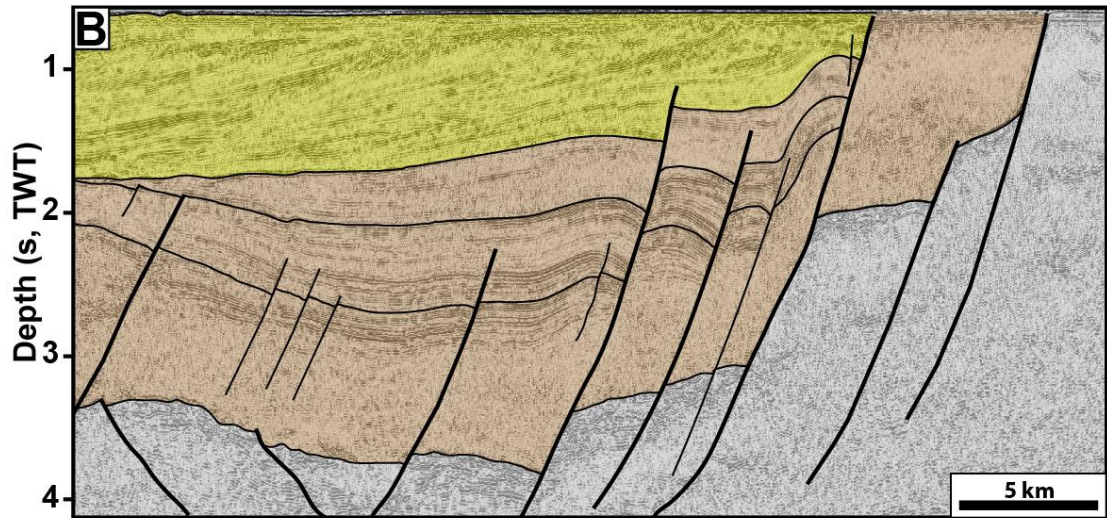
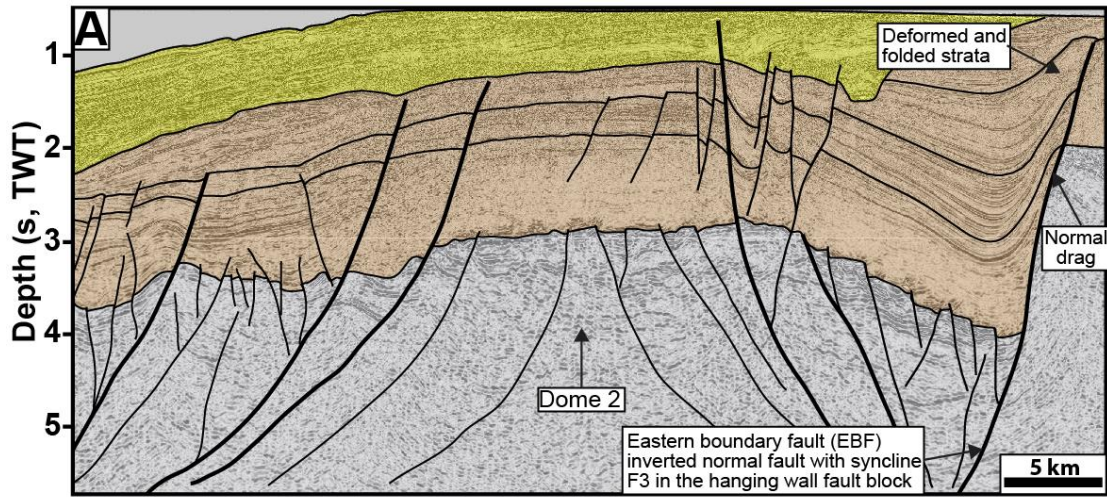
242 The data set of this study includes 2D seismic reflection data from several surveys and  
243 well data in the Vestbakken Volcanic Province. Data coverage is less dense in northern  
244 part of the study area. Typical spacing of seismic lines is 4km. Well 7316/5-1 was used  
245 to correlate the seismic data with formation tops in the study area whereas published  
246 paper based correlations provided calibration and age of each seismic horizon mapped  
247 (e.g. Eidvin et al., 1993; 1998 Ryseth et al., 2003). Three stratigraphic groups are  
248 present in the well; the Nordland Group (473 - 945 m); the Sotbakken Group (945-  
249 3752m) and Nygrunnen Group (3752-4014m) (Eidvin et al., 1993; 1998;  
250 [www.npd.com](http://www.npd.com)). Several folds of regional significance and with axial traces that can be  
251 followed along strike for 2-3 km or more occur in the Vestbakken Volcanic Province.  
252 The folds commonly are situated in the hanging walls of extensional faults and the fold  
253 traces and the structural grain of the thick-skinned master faults are generally parallel.  
254 This shows that the position and orientation of the folds were determined by the  
255 preexisting structural fabric affiliated with these faults. The continuity of the folds  
256 remains obscure due to spacing of reflection seismic lines, so each fold may include  
257 undetected overlap zones or axial off-sets that have not been detected. The folds were  
258 identified on the lower Eocene, Oligocen and lower Miocene levels. All the mapped  
259 folds are either positioned in the hanging walls of extensional (sometimes inverted)  
260 master faults or are dissected by younger faults with minor throws.

261

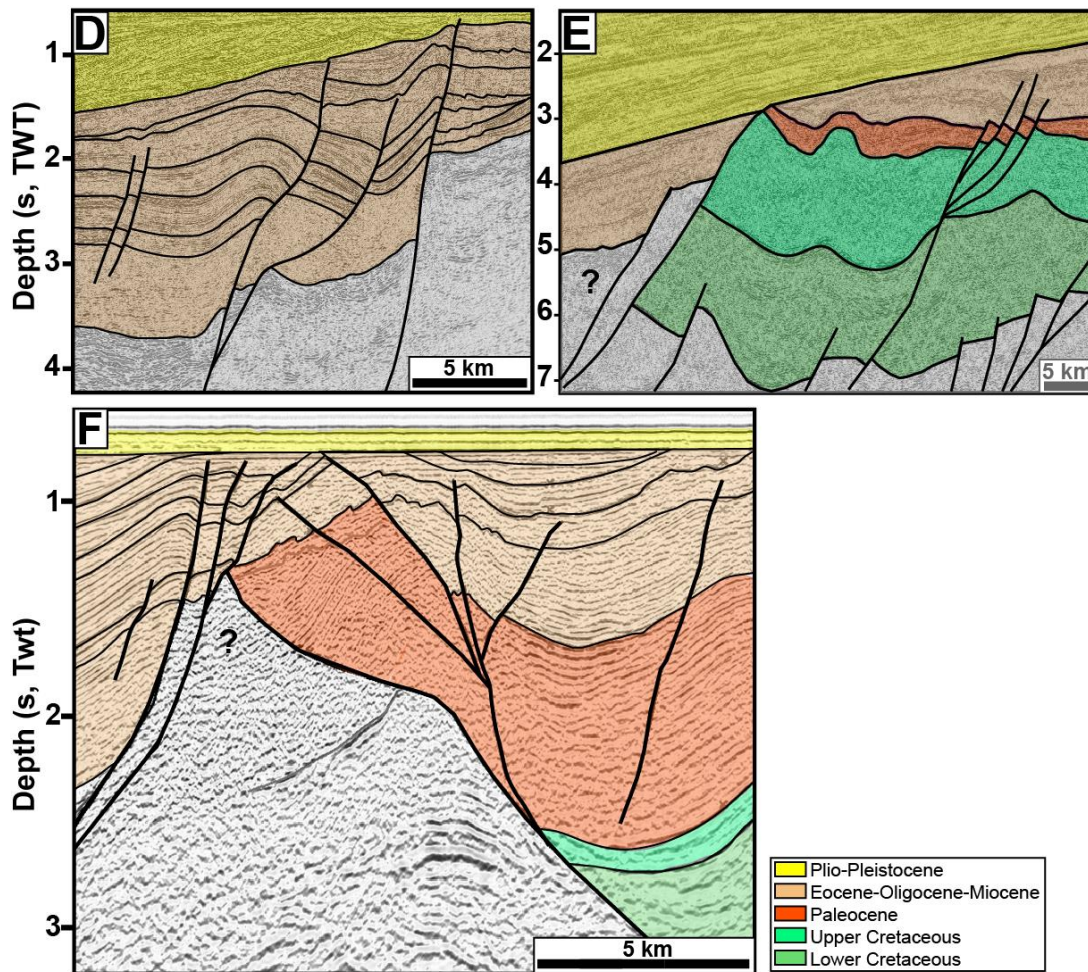
262

263





264  
265  
266



267

268 **Figure 2:** Seismic examples, Vestbakken Volcanic Province. **A)** Gentle, partly  
 269 collapsed NE-SW-striking anticline/dome of uncertain origin in the eastern  
 270 terrace domain of the southern Vestbakken Volcanic Province. **B,C)** Asymmetrical  
 271 folds (fold family 2; Giannenas 2018) situated along the eastern margin of the  
 272 Vestbakken Volcanic Province. These may represent primary SPE-4-structures  
 273 focused in the hanging walls along margins of master fault blocks, representing  
 274 reactivated SPE-2-structures. **D)** trains of symmetrical folds with upright fold axes  
 275 (corresponding to PSE-5-structures are preserved inside larger fault blocks. See  
 276 text for explanation of SPE-structures. **E)** Section through push-up associated with  
 277 restraining bend (PSE-4-structure). **F)** Flower (PSE-2)-structure in area  
 278 dominated by neutral shear.

279

## 280 **Strike-slip systems and analogue shear experiments**

281 Shear margins and strike-slip systems are structurally complex and highly  
 282 dynamic, so that the eventual architecture of such systems include structural  
 283 elements that were not contemporaneous (e.g. Graymer et al., 2007; Crowell,  
 284 1962; 1974a,b; Woodcock & Fischer, 1986; Mousloupoulou et al., 2007; 2008).  
 285 Analogue models offer the option to study the dynamics of such relations and  
 286 therefore attracted the attention of early workers in this field (eg. Cloos 1928;

287 Riedel 1929) and have continued to do so until today. Early experimental works  
288 mostly utilized one-layer (“Riedel-box”) models (e.g. Emmons 1969; Tchalenko,  
289 1970; Wilcox et al., 1973), which were soon to be expanded by the study of  
290 multilayer systems (e.g. Faugère et al., 1986; Naylor et al., 1986; Richard et al.,  
291 1991; Richard & Cobbold, 1989, 1995; Schreurs, 1994, 2003; Manduit & Dauteuil,  
292 1996; Dateuil & Mart, 1998; Schreurs & Colletta, 1998, 2003; Ueta et al., 2000;  
293 Dooley & Schreurs, 2012). The systematics and dynamics of strike-slip systems  
294 have been focused upon in a number of summaries like Sylvester (1985; 1988);  
295 Biddle & Christie-Blick (1985a,b); Cunningham & Mann (2007); Dooley &  
296 Schreurs (2012); Nemcok et al. (2016) and Peacock et al. (2016). Concepts and  
297 nomenclature established in these works are used in the following descriptions  
298 and analysis. Also, following Christie-Blick & Biddle (1985a,b) and Dooley &  
299 Schreurs (2012) we apply the term Principal Deformation Zone (PDZ) for the  
300 junction between the movable polythene plates underlying the experiment. The  
301 contact between the fixed and movable base defined a non-stationary velocity  
302 discontinuity (“VD”; Ballard et al., 1987; Allemand & Brun, 1991; Tron & Brun,  
303 1991).

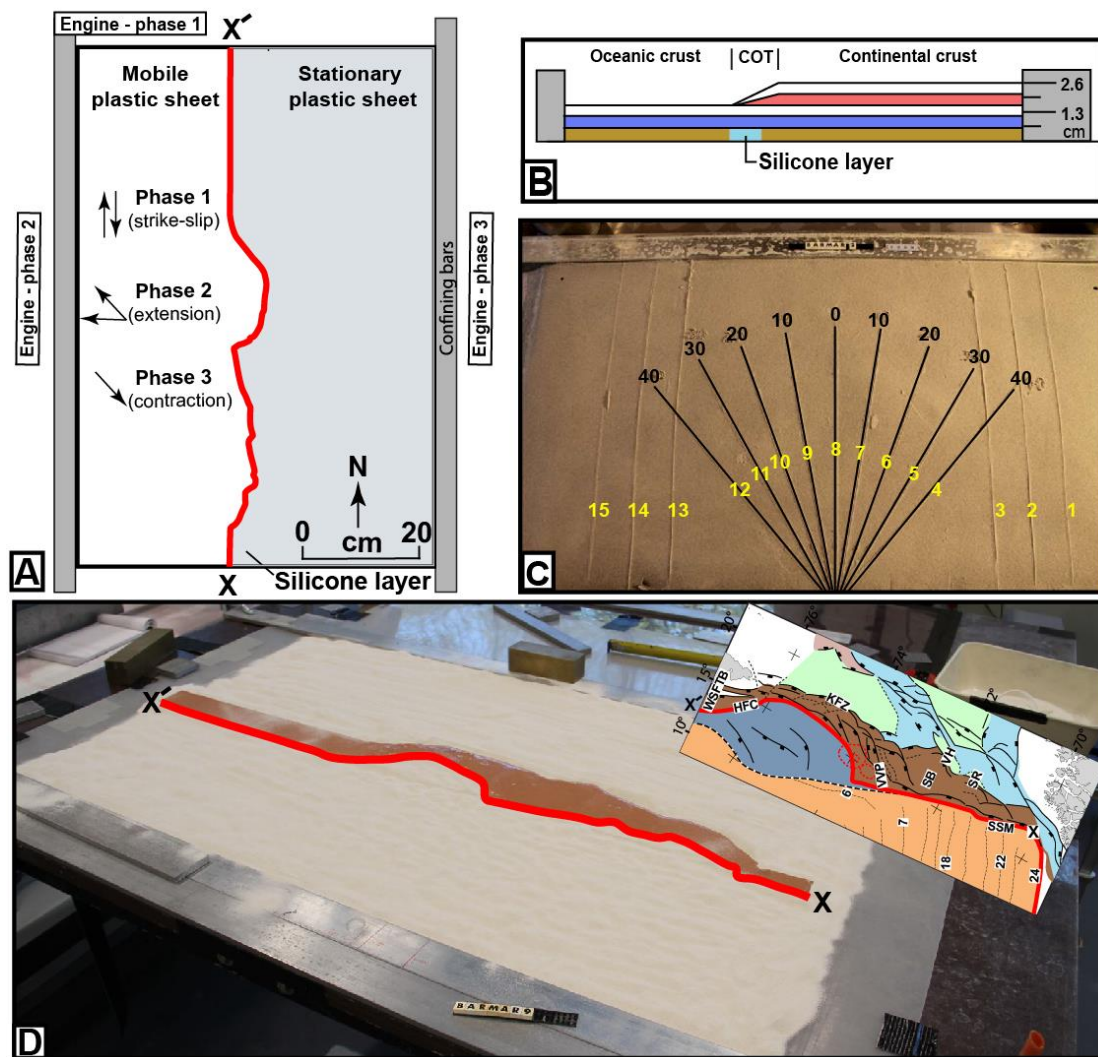
304 Several experimental works have particularly focused on the geometry and  
305 development of pull-apart-basins in releasing bend settings (Mann et al., 1983;  
306 Faugère et al. 1983; Richard et al. 1995; Dooley & McClay 1997; Basile & Brun  
307 1999; Sims et al., 1999; Le Calvez & Vendeville, 2002; Mann, 2007; Mitra & Paul,  
308 2011). The pull-apart basin was described by Burchfiel & Stewart (1966) and  
309 Crowell (1974a,b) as formed at a releasing bend or at a releasing fault step-over  
310 along a strike-slip zone (Biddle & Christie-Blick 1985a,b). This basin type has also  
311 been termed “rhomb grabens” (Freund, 1971) and “strike-slip basins” (Mann et  
312 al., 1993) and is commonly considered to be synonymous with the extensional  
313 strike-slip duplex (Woodcock & Fischer, 1986; Dooley & Schreurs, 2012). In the  
314 descriptions of our experiments, we found it convenient to distinguish between  
315 extensional strike-slip duplexes in the context of Woodcock & Fischer (1986) and  
316 Twiss & Moores, 2007, p. 140-141;) and pull-apart basins (rhomb grabens:  
317 Crowell, 1974a,b; Aydin & Nur, 1993) since they reflect slightly different stages in  
318 the development in our experiments (see discussion).

## 319 **Experimental setup**

320 To study the kinematics of complex shear margins, a series of analogue  
321 experiments were performed at the tectonic modelling laboratory (TecLab) of  
322 Utrecht University, The Netherlands. All experiments were built on two  
323 overlapping 1 mm thick plastic sheets (each 100 cm long and 50 cm wide) that  
324 were placed on a flat, horizontal table surface. The boundary between the  
325 underlying movable and overlaying stationary plastic sheets had the shape of the  
326 mapped continent-ocean boundary (COB; **Figure 1B**). The moveable sheet was  
327 connected to an electronic engine, which pulled the sheet at constant velocity  
328 during all three deformation stages. Displacement rates were therefore not scaled.  
329 The modelling material was then placed on these sheets where the layers on the  
330 stationary sheet represent the continental crust including the continent-ocean  
331 transition (COT) whereas those on the mobile sheet represents the oceanic crust.  
332 The model layers were confined by aluminum bars along the long sides and sand  
333 along the short sides (**Figure 3A**). The continental crust tapers off towards the  
334 oceanic crust with a relatively constant gradient. A sand-wedge with a constant  
335 dip angle determined by the difference in thickness between the intact and the  
336 stretched crust, and that covered the width of the silicon putty layer, was made to  
337 simulate the ocean-continent transition (**Figure 3B**). The taper angle was kept  
338 constant for all models.

339 The pre-cut shape of the plate boundary includes major releasing bends  
340 positioned so that they correspond to the geometry of the COB and the three main  
341 structural segments of the Barents Shear Margin as follows. *Segment 1* of the  
342 BarMar-experiments (**Figure 4**) contained several sub-segments with releasing  
343 and restraining bends as well as segments of “neutral” (Wilcox et al., 1973; Mann  
344 et al. 1983; Biddle & Christie-Blick, 1985b) or “pure” (Richard et al., 1991) strike-  
345 slip. *Segment 2* had a basic crescent shape, thereby defining a releasing bend at its  
346 southern margin in the position similar to that of the Vestbakken Volcanic  
347 Province, that merged into a neutral shear-segment along the strike of, whereas a  
348 restraining bend occupied the northern margin of the segment. *Segment 3* was a  
349 straight basement segment, defining a zone of neutral shear and corresponds to  
350 the strike-slip segment west of Svalbard (**Figure 1**).

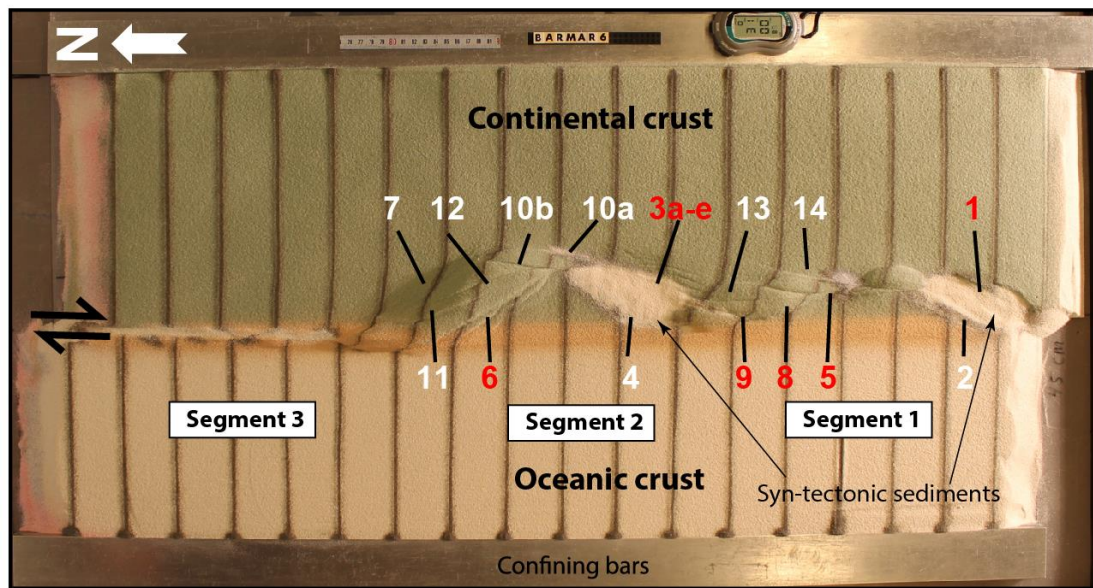
351



352

353 **Figure 3:** **A)** Schematical set-up of BarMar3-experiment as seen in map view. **B)**  
 354 Section through same experiment before deformation, indicating stratification  
 355 and thickness relations. **C)** Standard positions and orientation for sections cut in  
 356 all experiments in the BarMar-series. Yellow numbers are section numbers. Black  
 357 numbers indicate angle between the margins of the experiment (relative to N-S)  
 358 for each profile. **D)** Outline of silicone putty layer as applied in all experiments.  
 359 Inset shows original structural map of the Barents Margin used to define the width  
 360 of the thinned crust. Red line (X-X') indicates the western limit of the thinned zone.  
 361

362 The experiments included three stages of deformation with constant rates of  
 363 movement of the mobile sheet at  $10 \text{ cm hr}^{-1}$  in all three stages. The relative angles  
 364 of plate movements in the experiments were taken from post late Paleocene  
 365 opening directions in the northeast Atlantic (Gaina et al. 2009). Dextral shear was  
 366 applied in the *first phase* in all experiments by pulling the lower plastic sheet by  
 367 5cm. In the *second phase* the left side of the experiment was extended by 3 cm  
 368 orthogonally (BarMar6) or obliquely (315 degrees; BarMar 8 & 9) to the trend of



369

370 **Figure 4:** Position of segments and major structural elements as referred to in the  
 371 text and subsequent figures (see particularly **Figures 5 and 6**). This example is  
 372 taken from the reference experiment BarMar6. All experiments BarMar6-9  
 373 followed the same pattern, and the same nomenclature was used in the  
 374 description of all experiments and provides the template for the definition of  
 375 structural elements in Figure 7. Color code for numbers: Red: Faults that were  
 376 initiated as normal fault. White: faults that were activated as shear faults.  
 377

378 the shear margin, whereas plate motion was reversed during the *third phase of*  
 379 *deformation*, leading to inversion of earlier formed basins that had been  
 380 developed in the strike-slip and extensional phases. Sedimentary basins that  
 381 develop due to strike-slip (phase 1) or extension (phase 2) have been filled with  
 382 layers of colored feldspar sand by sieving, so that a smooth surface was obtained.  
 383 These layers are primarily important for discriminating among deformation  
 384 phases and thus act as marker horizons. Phase 3 was initiated by inverting the  
 385 orthogonal (BarMar6) or oblique (BarMar 8 & 9) extension of Phase 2 to  
 386 contraction as a proxy for ridge-push that likely was initiated when the mid-  
 387 oceanic ridge was established in Miocene time in the North Atlantic (Moser et al.,  
 388 2002; Gaina et al., 2009). Contraction generated by ridge-push has been inferred  
 389 from the mid Norwegian continental shelf (Våagnes et al., 1998; Pascal & Gabrielsen,  
 390 2001; Faleide et al., 2008; Gac et al., 2016) and seems still to prevail in the  
 391 northern areas of Scandinavia (Pascal et al., 2005), although far-field compression  
 392 generated by other processes have been suggested (eg. Doré & Lundin, 1996).

393 Coloured layers of dry feldspar sand represent the brittle oceanic and continental  
394 crust. This material has proven suitable for simulating brittle deformation  
395 conditions (Willingshofer et al., 2005; Luth et al., 2010; Auzemery et al., 2021) and  
396 is characterized by a grain size of 100-200 $\mu\text{m}$ , a density of 1300  $\text{kgm}^{-3}$ , a cohesion  
397 of  $\sim 16\text{-}45$  Pa and a peak friction coefficient of 0.67 (Willingshofer et al., 2018).  
398 Additionally, a 8 mm thick and of variable width corresponding to the transition  
399 zone (as mapped in reflection seismic data) of 'Rhodorsil Gomme GSIR' (Sokoutis,  
400 1987) silicone putty mixed with fillers was used as a proxy for the thinned and  
401 weakened continental crust at the ocean-continent transition (**Figure 1B and**  
402 **3A,B**). This Newtonian material ( $n=1.09$ ) has a density of 1330  $\text{kgm}^{-3}$  and a  
403 viscosity of  $1.42 \times 10^4$  Pa.s.

404 The experiments were scaled following standard scaling procedures as described  
405 by Hubbert (1937), Ramberg (1967) or Weijermars and Schmeling (1986),  
406 assuming that inertia forces are negligible when modelling tectonic processes on  
407 geologic timescales (see Ramberg (1981) and Del Ventisette et al. (2007) for a  
408 discussion on this topic). The models were scaled so that 10 mm in the model  
409 approximates c. 10 km in nature yielding a length scale ratio of  $1.00 \times 10^{-6}$ . As such,  
410 the model oceanic and continental crusts scale to 18 and 26 km in nature,  
411 respectively, which, although slightly overestimating the most intensely thinned  
412 oceanic crust (10-12 km) is in full agreement with the estimated thickness of the  
413 thinned oceanward segment of the continental crust (30-20 km Breivik et al.,  
414 1998).

415 The brittle crust, dry feldspar sand, deforms according to the Mohr-Coulomb  
416 fracture criterion (Horsfield, 1977; Mandl et al., 1977; McClay, 1990; Richard et  
417 al., 1991; Klinkmüller et al., 2016), whereas silicone putty promotes ductile  
418 deformation and folding. The geometry applied in the present experiments is  
419 accordingly well suited for the study of the COB in the Barents Shear Margin  
420 (Breivik et al., 1998).

421 When complete, the experiments were covered with a thin layer of sand further to  
422 stabilize the surface topography before the models were saturated with water and  
423 cross-sections that were oriented transverse to the velocity discontinuity were cut  
424 in a fan-shaped pattern (**Figure 3C**). All experiments have been monitored with a  
425 digital camera providing top-view images at regular time intervals of one minute.

426 All experiments performed were oriented in a N-S-coordinate framework to  
427 facilitate comparison with the western Barents Sea area and had a three-stage  
428 deformation sequence (dextral shear – extension – contraction). All descriptions  
429 and figures relate to this orientation. It was noted that all experiments reproduced  
430 comparable basic geometries and structural types, demonstrating robustness  
431 against variations in contrasting strength of the “ocean-continent”-transition  
432 zone, which included by a zone of silicone putty with variable width below an  
433 eastward thickening sand-wedge (**Figure 3B**) and changing displacement  
434 velocities. The experiments were terminated before the full closure of the basin  
435 system, in accordance with the extension vector > contraction vector as in the  
436 North Atlantic (see Vågnes et al. 1998; Pascal & Gabrielsen 2001; Gaina et al.  
437 2009).

438

### 439 **Modelling Results**

440 A series of nine experiments (BarMar1-9) with the set-up described above was  
441 performed. Experiments BarMar1-5 were used to calibrate and optimize  
442 geometrical outline, deformation rate, and angles of relative plate movements and  
443 are not shown here. The optimized geometries and experimental conditions were  
444 utilized for experiments BarMar6-9, of which BarMar6 and 8 (and some examples  
445 from BarMar9 and are illustrated here, yielded similar results in that all crucial  
446 structural elements (faults and folds) were reproduced in all experiments as  
447 described in the text are shown in **Figure 4.**) It is emphasized that the extensional  
448 basins affiliated with the extension phase (phase 2) became wider in the  
449 orthogonal (BarMar6) as compared to oblique extension experiments (BarMar 8)  
450 (**Figures 5 and 6**). Furthermore, the fold systems generated in the experiments  
451 that utilized oblique contraction of  $3145/135^0$  (BarMar8-9) produced more  
452 extensive systems of non-cylindrical folds with continuous, but more curved fold  
453 traces as compared experiments with orthogonal extension/contraction  
454 (BarMar6). The fold axes generally rotated to become parallel to the (extensional)  
455 master faults delineating the pull-apart basins generated in deformation stage 1  
456 in experiments with an oblique opening/closing angle.

457 Examples of the sequential development is displayed in **Figures 5 and 6**) and  
458 summarized in **Figure 7**.



459 Elongated positive structural elements with fold-like morphology as seen on the  
460 surface were detected during the various stages of the present experiments. The  
461 true nature of those were not easily determined until the experiments were  
462 terminated and transects could be examined. Such structures included buried  
463 push-ups (*sensu* Dooley & Schreurs, 2012), antiformal stacks, back-thrusts,  
464 positive flower structures, fold trains, and simple anticlines. For convenience, we  
465 use the non-genetic term “positive structural elements” termed *PSEm-n* for such  
466 structure types as seen in the experiments in the following description.

467 In the following the deformation in each segment is characterized for the three  
468 deformation phases (**Table 1**).

469

#### 470 **Deformation phase 1: Dextral shear stage**

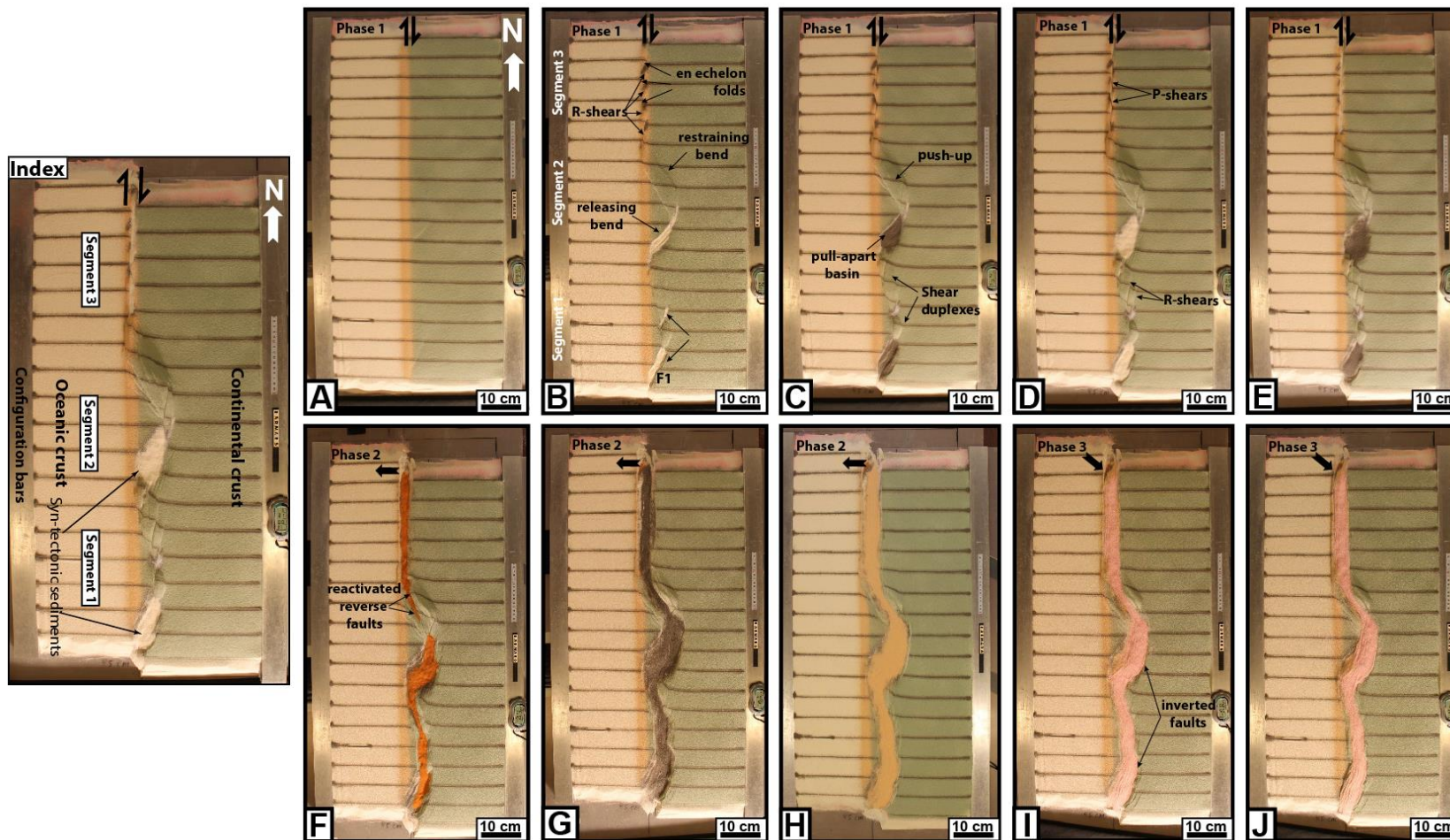
471 *Segment 1*: Differences in the geometry of the pre-cut fault trace between  
472 segments 1, 2 and 3 became evident after the very initial deformation stage.  
473 Particularly in segments 1 and 3 an array of oblique *en échelon* folds in between  
474 Riedel shear structures (*PSE-1-structures*) oriented c. 135°(NW-SE) to the regional  
475 VD rotating towards NNW-SSE by continued shear (**Figure 8**; see also Wilcox et  
476 al., 1973; Ordonne & Vialon, 1983; Richard et al., 1991; Dooley & Schreurs, 2012).  
477 These were simple, harmonic folds with upright axial planes and fold axial traces  
478 extending a few cm beyond the surface shear-zone described above. They had  
479 amplitudes on the scale of a few millimeters and wavelengths on scale of 5 cm. The  
480 *PSE-1-structures* interfered with or were dismembered by younger structures (Y-  
481 shears and *PSE-2-structures*; see below) causing northerly rotation of individual  
482 intra-fault zone lamellae (remnant *PSE-1-structures*; **Figure 8**). Structures similar  
483 to *PSE-1-fold* arrays are known from almost all strike-slip experiments reported  
484 and described in the literature from the early works (eg. Cloos, 1928; Riedel,  
485 1929. See Dooley & Schreurs, 2012 for summary) and are therefore not given  
486 further attention here.

487 By 0.25 cm of horizontal displacement in segment 1, which included releasing and  
488 restraining bends separated by a central strand of neutral shear, a slightly  
489 curvilinear surface trace of a NE-SW-striking, top-NW normal fault in the  
490 southernmost part of segment 1 developed. This co-existed with the *PSE-1-*  
491 *structures* and became paralleled by a normal fault with opposite dip (fault 2,

492 **Table 1**  
 493 Characteristics of Positive Structural Element (PSE 1-6) as described in the text and shown in figures. Note that the PSE-1-structures that  
 494 were developed in the earliest stages of the experiments became cannibalized during the continued deformation. No candidates of these  
 495 structures were identified in the reflection seismic sections..  
 496

Struct. type	Structural configuration	Orientation	Expr. stage	Segment	Recognized in seismic	Figure Expr	Figure Seism
PSE-1	Open syn-anticline system	135 deg	Stage 1	1,3	?	5,6	1A?
PSE-2	Incipient flower or half-flower	Parallel master fault	Stage 1	1,2,3	Yes	5,6,8	1B
PSE-3	Forced folds above rotated fault blocks	Parallel master fault in releasing bend	Stage 2	1,2	Yes	9B	
PSE-4	Push-up	Parallel master fault in restraining bend	Stage 1	2	Yes	9D	1C
PSE-5	Anticlines/snake-heads in hanging walls	Parallel master faults	Stage 3	1,2,3	Yes	9C,D	1D,E
PSE-6	Anticline-syncline trains	Parallel master faults	Stage 3	1,2,3	Yes	12	1F

497



498

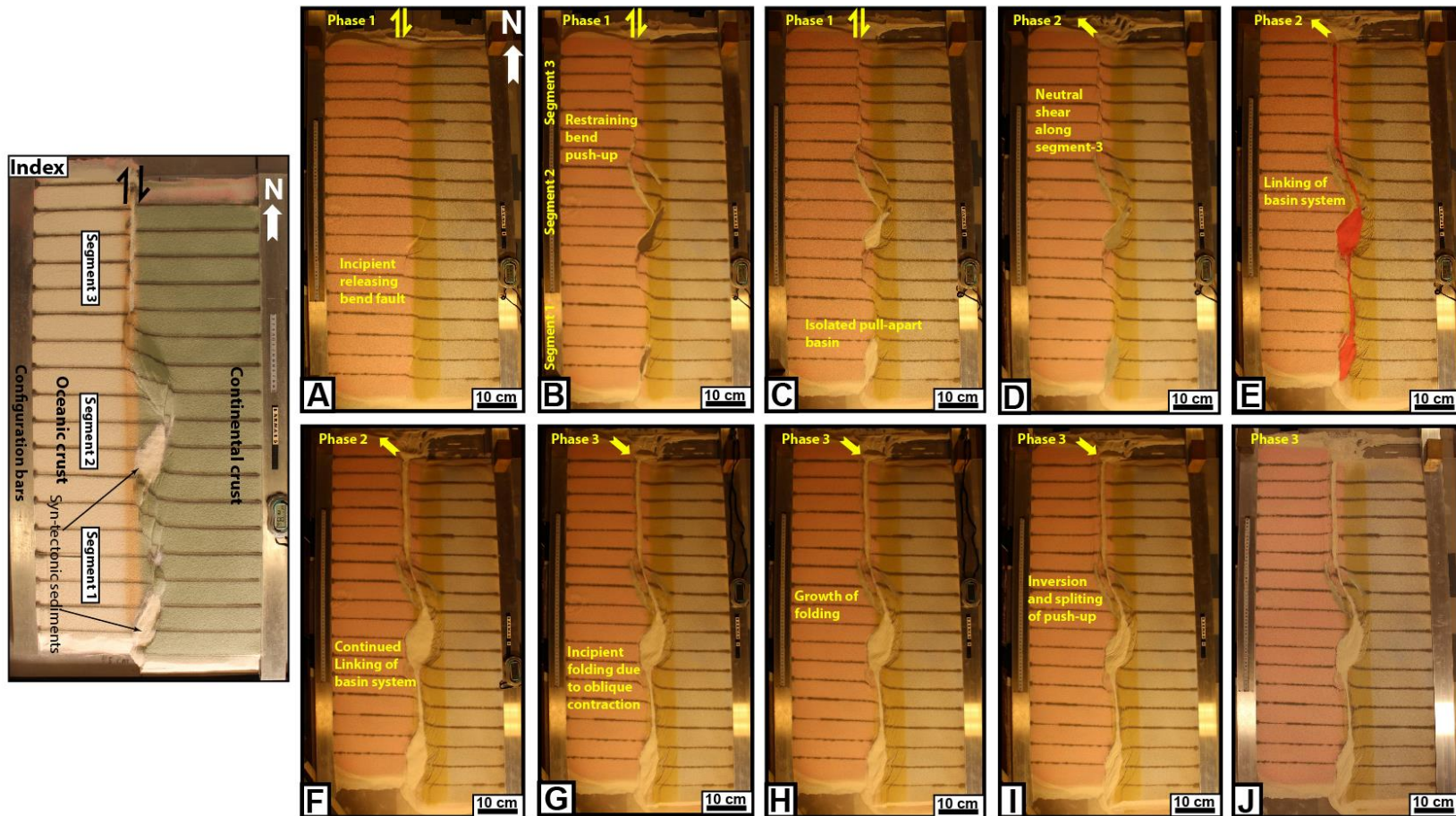
499 **Figure 5:** Sequential development of experiment BarMar6 by 0.5, 2.4, 3.5, 4.0 and 5.0 cm of dextral shear (Steps A-E), orthogonal extension  
 500 (steps F-H) and oblique contraction (steps I-J). The master fault strands are numbered in **Figure 4**, and the sequential development for  
 501 each structural family is shown in **Figure 7**. The reference panel to the left shows the positions of the segments. .

502 **Figure 4)** so that the two faults constrained a crescent- or spindle-shaped  
503 incipient extensional shear duplex (**Figures 5B and 6B**; see also Mann et al., 1983;  
504 Christie-Blick & Biddle, 1985; Mann 2007; Dooley & Schreurs, 2012).

505 A system of *en échelon* separate N-S to NNE-SSE- striking normal and shear fault  
506 segments became visible in segment 1 after ca. 1 cm of shear (**Figure 5C,D**). These  
507 faults did not have the orientations as expected for R (Riedel) - and R' (anti-  
508 Riedel)- shears (that would be oriented with angles of approximately 15 and 75°  
509 from the master fault trace) but became progressively linked with along strike  
510 growth and the development of new faults and fault segments. They thereby  
511 acquired the characteristics of Y-shears (oriented sub-parallel to the master fault  
512 trace), dissecting the PSE-1-structures. By 2.4 cm of shear, segment 1 had become  
513 one unified fault array (**Figure 5D and 6D**), delineating a system of incipient  
514 push-ups or positive flower structures (*PSE-2-structures*; **Figures 8 and Figure**  
515 **10, sections B1 and B3**).

516 The PSE-2-structures had amplitudes of 1 - 2 cm and wavelengths of 3 - 5 cm as  
517 measured on the surface with fault surfaces that steepened down-section, the  
518 deepest parts of the structures having cores of sand-layers deformed by open to  
519 tight folds. The folds had upright or slightly inclined axial planes, dipping up to  
520 55°, mainly to the east. The structures also affected the shallowest layers down to  
521 1-2 cm in the sequence, but the shallowest sequences were developed at a later  
522 stage of deformation and were characterized by simple gentle to open anticlines.  
523 These structures were constrained to a deformation zone directly above the trace  
524 of the basement fault, similar to that commonly seen along shear zones (e.g.  
525 Tchalenko, 1971; Crowell, 1974 a,b; Dooley & Schreurs, 2012). This zone was 3-4  
526 cm wide and remained stable throughout deformation stage 1 and was restricted  
527 to the close vicinity of the basement shear fault itself. A horse-tail-like fault array  
528 developed by ca. 3 cm of shear at the transitions between segments 1 and 2  
529 (**Figures 5B-D and 6B-D**).

530 The structuring in *Segment 2*; was ruled by the pre-cut crescent-shaped basement  
531 fault (velocity discontinuity) that caused the development of a releasing bend  
532 along its southern, and a restraining bend along its northern border (**Figure 11**).  
533 The first fault of fault array 3a-e in the southern part of Segment 2 (**Figure 4**) was  
534 activated after c. 0.15 cm of bulk horizontal displacement (**Figure 7**). It was



535

536 **Figure 6:** Sequential development of experiment BarMar8 by 0.5, 2.4, 3.5, 4.0 and 5.0 cm of dextral shear (Steps A-E), oblique extension  
 537 (steps F-H) and oblique contraction (steps I-J). The master fault strands are numbered in **Figure 3**, and the sequential development for  
 538 each structural family is shown in **Figure 7**. Phases 2 and 3 involved oblique ( $315^{\circ}$ ) extension and contraction in this experiment. The  
 539 reference panel to the left shows the positions of the segments.

540 situated directly above the southernmost pre-cut releasing bend, defining the  
541 margin of crescent-shaped incipient extensional strike-slip duplexes (in the  
542 context of Woodcock & Fischer, 1986, Woodcock & Schubert, 1994 and Twiss &  
543 Moores, 2007, p. 140-141). The developing basin got a spindle-shaped structure  
544 and developed into a basin with a lazy-S-shape (Cunningham & Mann, 2007; Mann,  
545 2007). The basin widened towards the east by stepwise footwall collapse,  
546 generating sequentially rotating crescent-shaped extensional fault blocks that  
547 became trapped as extensional horses in the footwall of the releasing bend  
548 (**Figure 11**). In the areas of the most pronounced extension the crestal part of the  
549 rotational fault blocks became elevated above the basin floor, generating ridges  
550 that influenced the basin floor topography and hence, the sedimentation. By  
551 continued rotation of the fault blocks and simultaneous sieving of sand the crests  
552 of the blocks became sequentially uplifted, generating forced folds (Hamblin,  
553 1965; Stearns, 1978; Groshong, 1989; Khalil & McClay, 2016) (**Figure 10A**). In the  
554 analysis we used the term *PSE-3-structures* for these features. Simultaneously an  
555 expanding sand-sequence became trapped in the footwalls of the master faults,  
556 defining typical growth-fault geometries.

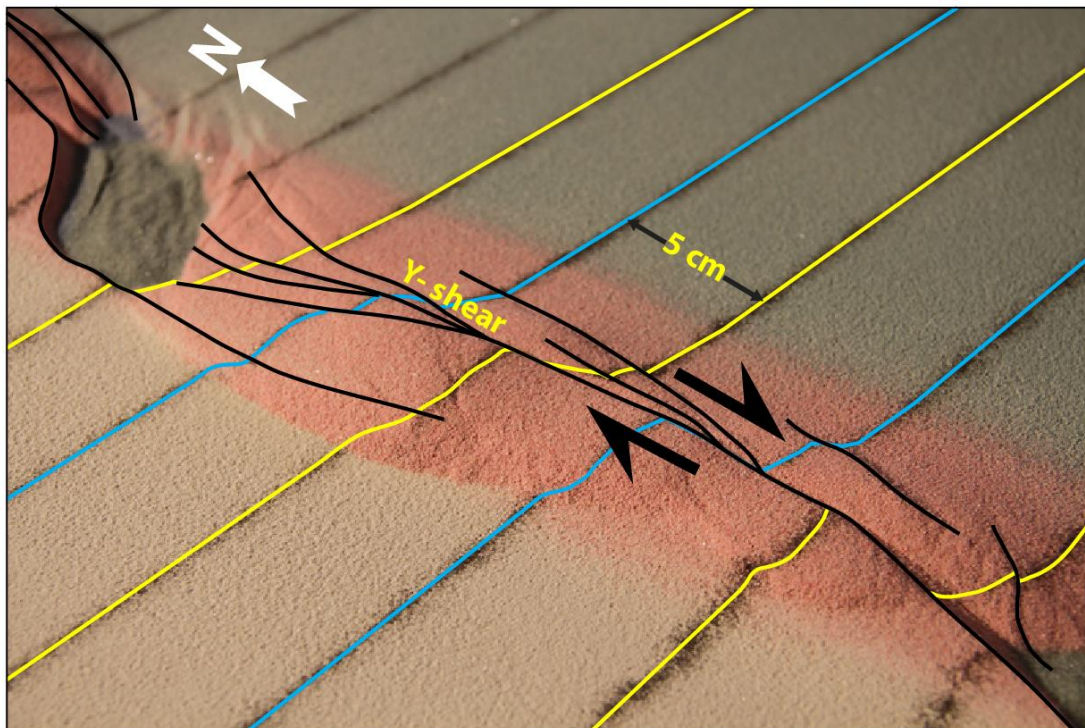
557 By a shear displacement of 0.55 cm additional curved splay faults were initiated  
558 from the northern tip of the master fault of fault 3f; **Figure 7**), delineating the  
559 northern margin of a rhombohedral pull-apart-basin (Mann et al., 1983; Mann,  
560 2007; Christie-Blick & Biddle, 1985) and with a geometry that was  
561 indistinguishable from pull-apart basins or rhomb grabens affiliated with  
562 unbridged *en échelon* fault arrays (Crowell, 1974 a,b; Aydin & Nur, 1993).  
563 Although sand was filled into the subsiding basins to minimize the graben relief  
564 and to prevent gravitational collapse, the sub-basins that were initiated in the  
565 shear-stage were affected by internal cross-faults, and the initial basin units  
566 remained the deepest so that the buried internal basin topography maintained a  
567 high relief with several apparent depo-centers separated by intra-basinal  
568 platforms.

569 Systems of linked shear faults and PSE-structures became established in the  
570 central part with neutral shear that separate the releasing and restraining bends  
571 and development similarly to that seen for segment 3 (see below), but these  
572 structures were soon destroyed by the combined development of the northern



578 and southern tips of the extensional and contractional shear duplexes (**Figure**  
579 **10**).

580 The first structure to develop in the regime of the restraining bend (segment 2;  
581 was a top-to-the-southwest (antithetic) thrust fault at an angle of  $145^{\circ}$  with the  
582 regional trend of the basement border as defined by segments 1 and 3 (Fault 6). It  
583 became visible by 0.5 cm of displacement. The northern part of segment 2 became,  
584 however, dominated by a synthetic contractional top-to-the-northeast fault that  
585 was initiated by 0.85 cm of shear (Fault 7 **Figures 5 and 6**). Thus, faults 6 and 7  
586 delineated a growing half-crescent-shaped 5-7-cm wide push-up structure (Aydin  
587 & Nur, 1982; Mann et al., 1983) south of the restraining bend (**Figure 9**; *PSE-4-*  
588 *structures*). By continued shear these structures got the character of an antiformal  
589 stack.



590

591 **Figure 8:** PSE-1 anticline-syncline pairs in segment 1 experiment BarMar6 in an  
592 oblique view (see Figure 4 for position of Segment 1). PSE-1 folds were  
593 constrained to the very fault zone and the fold axes (blue lines) and extended only  
594 3-4 cm beyond the fault zone. PSE-2 structures (incipient push-ups and positive  
595 flower structures; yellow lines) were delineated by shear faults and completely  
596 cannibalized PSE-1 structures by continued shear. Yellow and blue lines show the  
597 rotation of the fold axial trace caused by dextral shearing of c. 1,5 cm. 25mm of  
598 dextral shear. By a displacement of 35mm the remains of the PSE-1 structure was  
599 completely obliterated. The distance between the markers (dark lines) is 5cm.  
600 White arrow marks north-direction. Black arrows indicate shear direction.

601



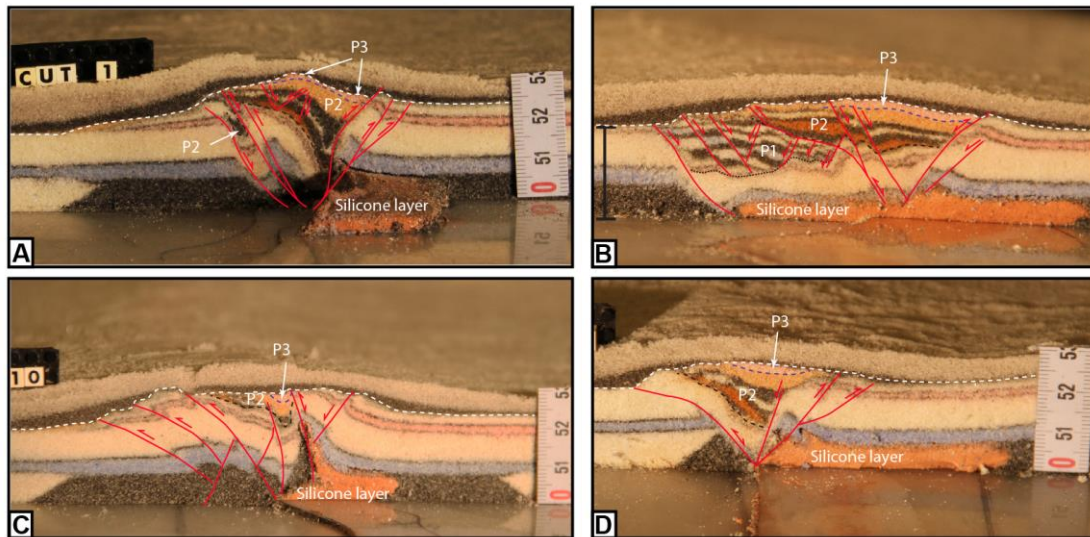
602 *Segment 3* defined a straight strand of neutral shear. Its development in the  
603 BarMar-experiments followed strictly that known from numerous published  
604 experiments (e.g. Tchalenko, 1970; Wilcox et al., 1973; Harding, 1974; Harding &  
605 Lowell, 1979; Naylor et al., 1986; Sylvester, 1988; Richard et al., 1991; Woodcock  
606 & Schubert, 1994; Dauteuil & Mart, 1998; Mann, 2007; Casas et al., 2001; Dooley  
607 & Schreurs, 2012). A train of Riedel-shears, occupying the full length of the  
608 segment, appeared simultaneously on the surface after a shear displacement of  
609 0.5 cm, occupying a restricted zone with a width of 2-3 cm. The Riedel-shears  
610 dominated the continued structural development of Segment 3. Riedel'-shears  
611 were absent throughout the experiments, as should be expected for a sand-  
612 dominated sequence (Dooley & Schreurs, 2012). P-shears developed by continued  
613 shear, creating linked rhombic structures delineated by the Riedel- and P-shears  
614 generating positive structural elements with NW-SE- and NNE-SSE-striking axes  
615 (see also Morgenstern & Tchalenko, 1967), soon coalescing to form Y-shears.  
616 Transverse sections document that these structures were cored by push-up  
617 anticlines, positive half-flower structures and full-fledged positive flower  
618 structures in the advanced stages of shear (*PSE-4-structures*) (**Figures 5 and 6.**  
619 **See also Figure 10**). These were accompanied by the development of *en échelon*  
620 folds and flower structures as commonly reported from strike-slip faults in nature  
621 and in experiments. The width of the zone above the basal fault remained almost  
622 constant throughout the experiments, but was somewhat wider in experiments  
623 with thicker basal silicone polymer layers, similar to that commonly described  
624 from comparable experiments (eg. Richard et al., 1991).

625

## 626 **Deformation Phase 2: Extension**

627 The late Cretaceous-Palaeocen dextral shear was followed by pure extension  
628 accompanying the opening along the Barents Shear Margin in the Oligocene. Our  
629 experiments focused on the effects of oblique extension, acknowledging that plate  
630 tectonic reconstructions of the North Atlantic suggest an extension angle of  $315^\circ$   
631 (Gaina et al., 2009).

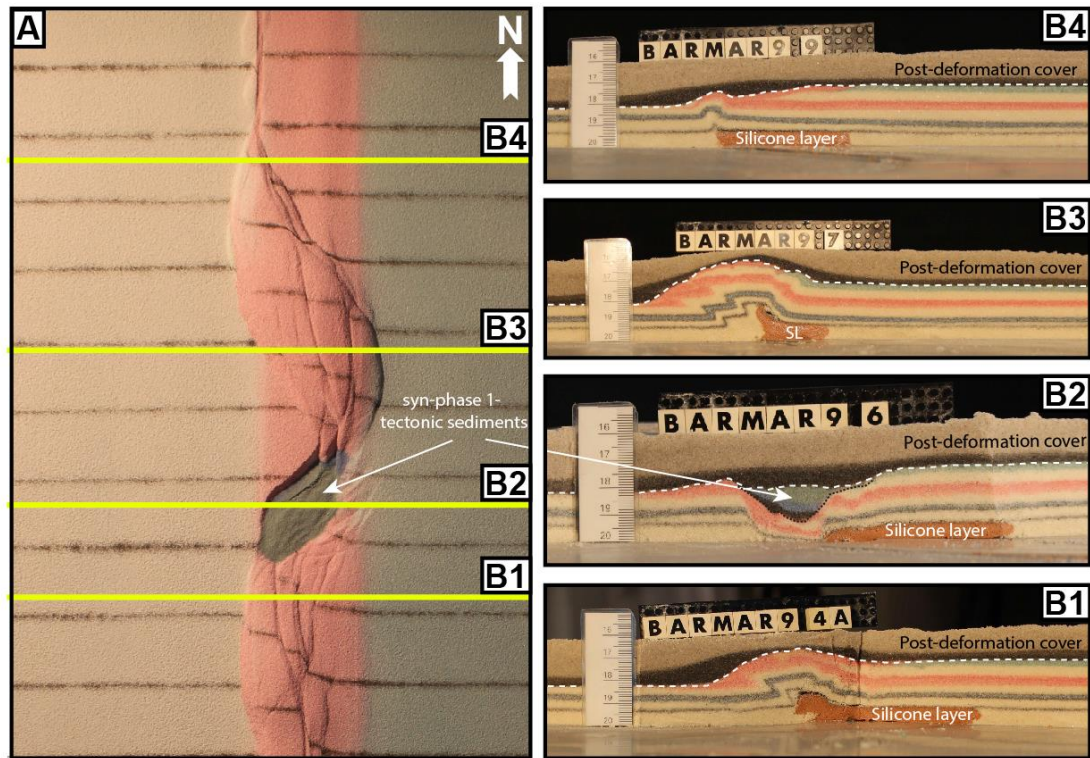
632 All strike-slip basins widened in the extensional stage, and as one would expect,  
633 the basins generated in orthogonal extension became wider than those generated  
634 in oblique extension. In both cases, however, extension promoted enhanced the



635

636 **Figure 9:** Cross-sections through PSE-2-related structures. PSE-structures are  
 637 marked with P and PSE-number (see also Table 1). **A)** Folded core of incipient  
 638 push-up/positive flower structure in segment 1, experiment BarMar6. The fold  
 639 structure is completely enveloped of shear faults that have a twisted along-strike  
 640 geometry. Note that the eastern margin of the structure developed into a negative  
 641 structure at a late stage in the development (filled by black-pink sand sequence)  
 642 and that the silicone putty sequence (basal pink sequence) was entirely isolated  
 643 in the footwall. **B)** Similar structure in experiment BarMar8. The weak silicone  
 644 putty layer here bridged the high-strain zone and focused folding that propagated  
 645 into the sand layers (blue). The folds in upper (pink layers) were associated with  
 646 the contractional stage, because they contributed to a surface relief filled in by red-  
 647 black-sand sequence that was sieved into the margin during the contractional  
 648 stage. **C)** Contraction associated with “crocodile structure” in the footwall of the  
 649 main fault in segment 1, experiment BarMar8. Note disharmonic folding with  
 650 contrasting fold geometries in hanging wall and footwall and at different  
 651 stratigraphic levels in the footwall, indicating shifting stress situation in time and  
 652 space in the experiment. **D)** Transitional fault strand between to more strongly  
 653 sheared fault segments (experiment BarMar9).  
 654

655 relief that had been generated in the shear-stage. In the earliest extensional stage  
 656 the strike-slip basin in segment 2 dominated the basin configuration, but by  
 657 continued extension the linear segments and the minor pull-apart basins in  
 658 segments 1 and 2 started to open and to become interlinked, subsequently  
 659 generating a linked basin system that runs parallel to the entire shear margin  
 660 (**Figures 5F-G, 6F-G**). The basins had become completely interlinked by an  
 661 extension of 1.25 cm (marked by the vertical dark blue line in **Figure 7**). The  
 662 orthogonal extension-phase also reactivated and linked several master faults that  
 663 were established in deformation phase 1 (**Figures 5A and 6A**). This became  
 664 evident by an extension of 0,25 – 0,50 cm and included the southern fault margin,



665

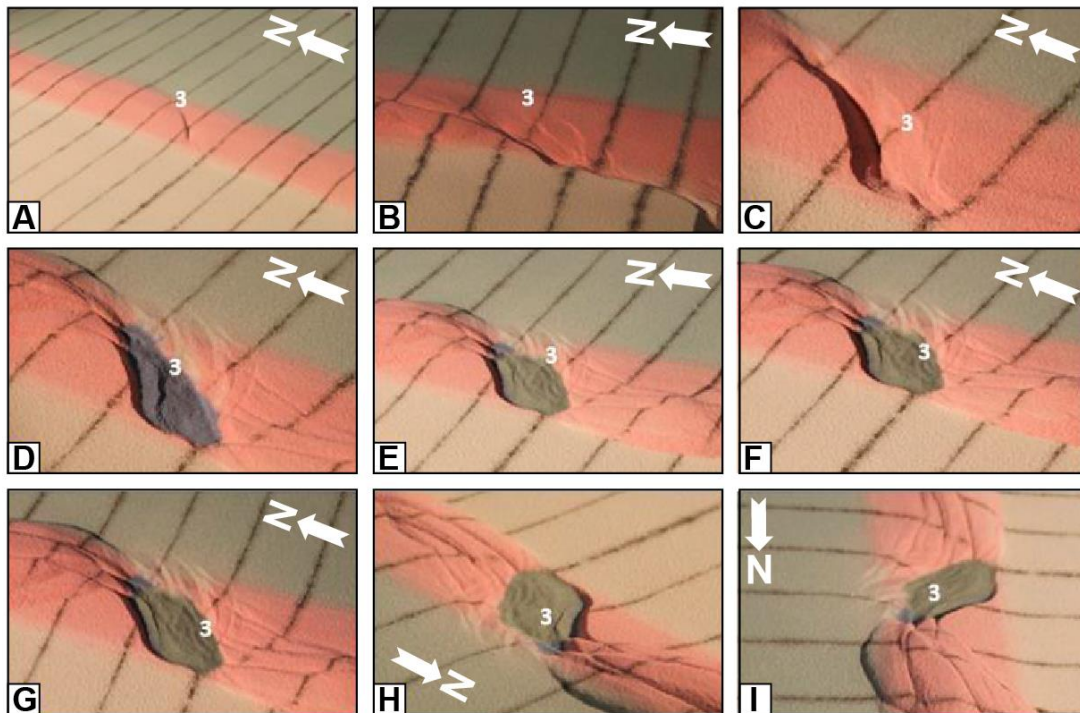
666 **Figure 10: A)** contrasting structural styles along the master fault system in  
 667 segment 2 in map view and **(B)** cross sections of experiment BarMar9. SL denotes  
 668 silicone layer, the stippled line the boundary between pre- and syn-deformation  
 669 layers and the white dashed line the boundary with the post-deformation layers.  
 670

671 the push-up and the splay faults defining the crestal collapse graben (Faults 6, 11  
 672 and 12; **Figure 4**). Among the faults that remained inactive throughout the  
 673 extension phase were the antithetic contractional fault delineating the push-ups  
 674 in segment 2 (Fault 6; **Figure 4**). The Y-shear in Segment 3 was reactivated as a  
 675 straight, continuous extensional fault in phase 2. Total extension in stage 2 was 5  
 676 cm.

677

### 678 **Deformation Phase 3: contraction**

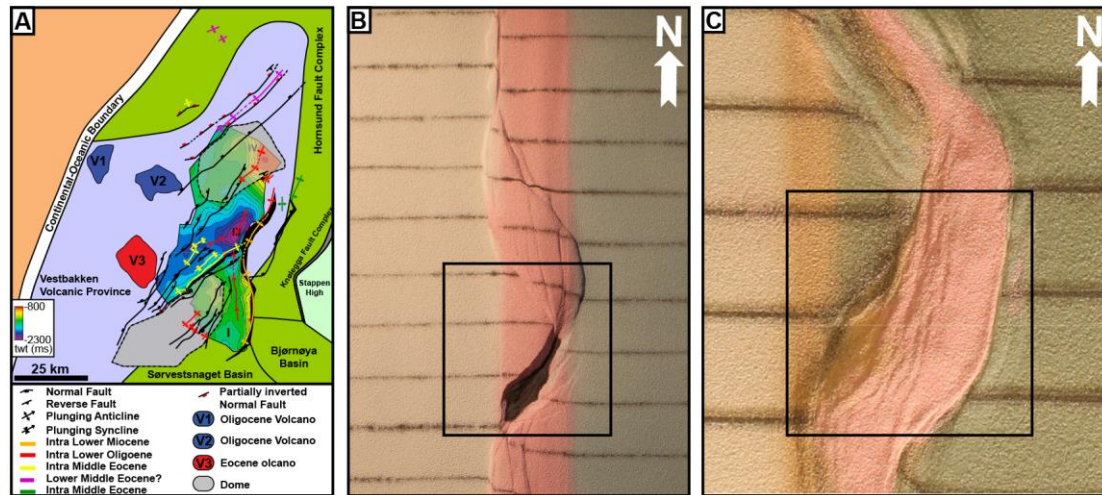
679 In our experiments the extension stage was followed by oblique contraction  
 680 (parallel to the direction of extension as applied for each experiment). A part of  
 681 the early-stage contraction was accommodated along new faults. It was more  
 682 common, however, that faults that had been generated in the strike-slip and  
 683 extensional stages became reactivated and rotated, and the development of  
 684 isolated folds, which were commonly associated with inverted fault traces,  
 685 generating snake-head or harpoon-structures structures (Cooper et al., 1989;



686

687 **Figure 11:** Nine stages in the development of the extensional shear duplex system  
 688 above the releasing bend in experiment BarMar9. The master faults that  
 689 developed at an incipient stage (e. Fault 3 that constrained the eastern margin of  
 690 the extensional shear duplex) remained stable and continued to be active  
 691 throughout the experiment (Figure 7), but became overstepped by faults in its  
 692 footwall that became the basin contraction faults at the later stages H and I. The  
 693 developing basement was stabilized by infilling of gray sand during this part of the  
 694 experiment. Fault 3 remained active and broke through the basin infill also after  
 695 the basin infill overstepped the original basin margin. The distance between the  
 696 markers (dark lines) is 5cm. Yellow arrow marks north-direction. Note that  
 697 figures “H” and “I” (bottom right) is viewed from directions that differs from the  
 698 other figures.  
 699

700 Coward, 1994; Allmendinger, 1998; Yameda & McClay, 2004; Pace & Calamitra,  
 701 2014); *PSE-5-structures*). The dominant structures affiliated with the contractional  
 702 stage was still new folds with traces oriented orthogonal to the shortening  
 703 direction and sub-parallel to the preexisting master fault systems that defined the  
 704 margin and basin margins (**Figure 12**). Also, some deep fold sets that had been  
 705 generated during the strike-slip phase and seen as domal surface features became  
 706 reactivated, causing renewed growth of surface structures (see **Figure 10** and  
 707 explanation in figure caption). These folds were generally up-right cylindrical  
 708 buckle folds in the initial contractional and with very large trace length:  
 709 amplitude-ratio (*SPE-6-structures*). Some intra-basin folds, however, defined fold



710

711 **Figure 12:** PSE-5-folds generated during phase 3-inversion, experiment BarMar8.  
 712 Note that fold axes mainly parallel the basin rims, but that they deviate from that  
 713 in the central parts of the basins in some cases. The folds are best developed in  
 714 segment 2, which accumulated extension in the combined shear and extension  
 715 stages.  
 716

717 arrays that diagonally crossed the basins. Particularly the folds situated along the  
 718 basin margins developed into fault propagation-folds above low-angle thrust  
 719 planes. Such faults aligning the western basin margins could have an antithetic  
 720 attitude relative to the direction of contraction.

721 During the contractional phase the margin-parallel, linked basin system started  
 722 immediately to narrow and several fault strands became inverted. The basin-  
 723 closure was a continuous process until the end of the experiment by 3 cm of  
 724 contraction. The contraction was initiated as a proxy for an ESE-directed ridge-  
 725 push stage. The first effect of this deformation stage was heralded by uplift of the  
 726 margin of the established shear zone that that had developed into a rift during  
 727 deformation stage 2. This was followed by the reactivation and inversion of some  
 728 master faults (eg. fault a2; eg. **Figure 4**) and thereafter by the development of a  
 729 new set of low-angle top-to-the-ESE contractional faults. These faults displayed a  
 730 sequential development, (fault family 1; **Figure 7**) and were associated with  
 731 folding of the strata in the rift structure, probably reflecting foreland-directed in-  
 732 sequence thrusting (SPE-5 and PSE-6 fold populations).

733

734

735

## 736 **Discussion**

737 The break-up and subsequent opening of the Norwegian-Greenland Sea was a  
738 multi-stage event (**Figure 13**) that imposed shifting stress configurations  
739 overprinting the already geometrically complex Barents Shear Margin. Therefore,  
740 scaled experiments were designed to illuminate its structural development. The  
741 experiments utilized three main segments that correspond to the Senja Fracture  
742 Zone (segment 1), the Vestbakken Volcanic Province (segment 2) and the  
743 Hornsund Fault Zone (segment 3) respectively and three deformation phases  
744 (dextral shear, oblique coextension and contraction). Several structural families  
745 (PSE 1-6) generated in the experiments correspond to structural features  
746 observed in reflection seismic sections. In the following discussion we utilize  
747 these two data sets in explaining the sequential development of each segment of  
748 the shear margin.

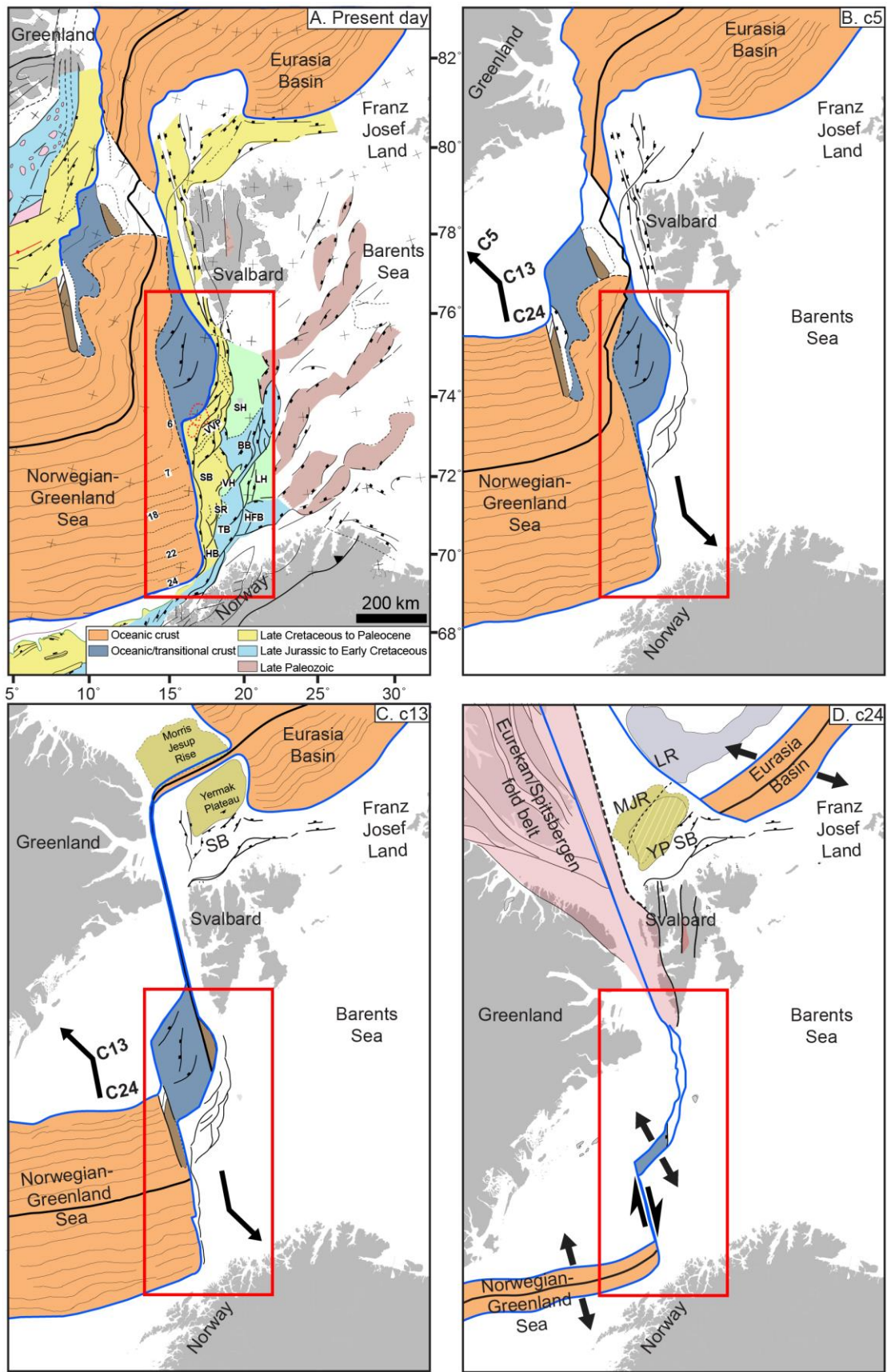
749

### 750 **Structures of phase 1 (dextral shear)**

751 *Segment 1* in the experiments (which corresponds to the Senja Fracture Zone) was  
752 dominated by neutral dextral shear, although jogs in the (pre-cut) fault provided  
753 minor sub-segments with subordinate releasing and restraining bends.

754 PSE-1-folds seen in the incipient shear phase were confined to the area just  
755 above the basal master fault (VD) and its immediate vicinity (see also experiments  
756 in series “e” and “f” of Mitra & Paul, 2011). Counterparts to PSE-1 structural  
757 population were not identified in the seismic data, although some isolated, local  
758 anticlinal features could be dismembered remnants of such. Because of their  
759 constriction to the near vicinity of the master fault it is reasonable that structures  
760 generated at an early stage of shear are vulnerable to cannibalization by younger  
761 structures with axes striking parallel to the main shear fault (Y-shears; SPE-2-  
762 structures). We therefore conclude that this structure population was destroyed  
763 during the later stages of shear and during the subsequent stages of extension and  
764 contraction.

765 PSE-1-folds, that developed at an incipient stage were immediately pursued by the  
766 development of two sets of NNE-SSW-striking normal faults with opposite throws  
767 in the releasing bend areas (eg. fault 2 **Figure 4**). The two faults defined crescent-  
768 or spindle-shaped incipient extensional shear duplexes. These structures were



769

770

771

772

**Figure 13;** Main stages in opening of the North Atlantic. The figure builds on figure 5 in Faleide et al. (2008) and has been updated and redrawn.

773 stable during the remainder of the experiments and their master faults became  
774 reactivated during the extensional and contractional phases (see below). The  
775 most prominent of these structures corresponds to the position of the  
776 Sørvestsnaget Basin (**Figure 1B**).

777 *Segment 2*, which was controlled by a pre-cut crescent-shaped discontinuity in  
778 the experiments corresponds to the Vestbakken Volcanic Province and the  
779 southern extension of the Knølegga Fault Complex of the Barents Shear Margin  
780 (**Figures 1b and 4**). The Vestbakken Volcanic Province is dominated by  
781 interfering NNW-SSE- and NE-SW striking fold- and fault systems in its central  
782 part, whereas N-S-structures are more common along its eastern margin (**Figure**  
783 **12A**) (Jebsen & Faleide, 1998; Giannenas, 2018). Intra-basinal highs and other  
784 internal configurations seen in the BarMar-experiments mainly reflect step-wise  
785 collapse of the intrinsic basin that generated rotational fault blocks, the crests of  
786 which separated local sediment accumulations. Such structures common in  
787 strike-slip basins (eg. Dooley & McClay, 1997; Dooley & Schreurs, 2012) and are  
788 consistent with the intra-basin depo-centers seen within the Vestbakken Volcanic  
789 province and in the Sørvestsnaget Basin as well (Knutsen & Larsen, 1997; Jebsen  
790 & Faleide, 1998; **Figure 13**). The crests of the rotating fault blocks are termed PSE-  
791 3-structures above, and such eroded fault block crests are defining the footwalls  
792 of major faults in the Vestbakken Volcanic Province, providing space for sediment  
793 accumulation in the footwalls. The area that was affected by the basin formation  
794 in the extensional shear duplex stage seems to have remained the deepest part of  
795 the Vestbakken Volcanic Province, whereas the part formed in basin widening by  
796 sequential footwall collapse created a shallower sub-platform (*sensu* Gabrielsen,  
797 1986) (**Figure 11**).

798 The Knølegga Fault Complex occupies a km-wide zone in segment 2. The master  
799 fault strand is paralleled by faults with significant normal throws on its hanging  
800 wall side and this belongs to the larger Knølegga Fault Complex (EBF; Eastern  
801 Boundary Fault; Giannenas, 2018; **Figure 12A**). The EBF zone is a top-west  
802 normal fault with maximum throw of nearly 2000 m (3000 meters). It can be  
803 followed along its strike for more than 60 km and seems to die out by horse-tailing  
804 at its tip-points. The vicinity of the master faults of the Knølegga Fault Complex  
805 locally display isolated elongate positive structures constrained by steeply



806 dipping faults. These structures sometimes display internal reflection patterns  
807 that seem exotic in comparison to the surrounding sequences. Some of these  
808 structures resemble positive flower structures or push-ups or define narrow  
809 anticlines. They are found in both the footwall and hanging wall of the border  
810 faults and strike parallel to those and the axes of these structures parallel the  
811 master faults. The traces of such structures can be followed over shorter distances  
812 than the master faults, and do not occur in the central parts of the Vestbakken  
813 Volcanic Province. We suggest that the composite geometry of the Knølegga Fault  
814 Complex is due to the development of PSE-2-structures within the realm of a pre-  
815 existing normal fault zone.

816 Due to the right-stepping geometry during dextral shear in segment 2, the  
817 southern and northern parts were in the releasing and restraining bend positions,  
818 respectively (eg. Christie-Blick & Biddle, 1985). Hence, the southern part of  
819 segment 2 was subject to oblique extension, subsidence and basin formation when  
820 the northern part was subject to oblique contraction, shortening and uplift. The  
821 southern segment expanded to the east and northeast by footwall collapse and  
822 activation of rotating fault blocks that contributed to a basin floor topography that  
823 affected the pattern of sediment accumulation (**Figure 9A, B**).

824

825 The positive structural elements that prevail in *segment 3* belong to the PSE-2-  
826 structure population. The structures affiliated with segment 3 in the BarMar-  
827 experiments are similar to those seen in the reflection seismic sections along parts  
828 of the Spitsbergen and the Senja shear margins (Myhre, et al. 1982) and elsewhere  
829 (Cloos, 1928; Riedel, 1929; Tchalenko, 1970; Wilcox et al., 1973). In the  
830 experiments *en echelon* folds (corresponding to PSE-1-structures) first became  
831 visible, to be succeeded by the development of Riedel- and P-shears (R'-shears  
832 were subdued as expected for sand-dominated sequences (Dooley & Schreurs,  
833 2012). Continued shear followed by collapse and interaction between Riedel and  
834 P-shears and the subsequent development of Y-shears initiated push-up- and  
835 flower-structure with N-S-axes (PSE-2) structures that were expressed as non-  
836 cylindrical (double-plunging) anticlines on the surface (eg. Tchalenko, 1970;  
837 Naylor et al., 1986). Structures similar to the PSE-2-structures that were initiated  
838 in the present experiments are common in scaled experiments with mechanically

839 stratified sequences where viscous basal strata are covered by sand (e.g. Richard  
840 et al., 1991; Dauteuil & Mart, 1998).

841

### 842 **Structures of phase 2 (extension)**

843 It is expected that (regional) basin and (local) fault block subsidence became  
844 accelerated during phase 2 (extension), and more so in the orthogonal extension  
845 experiments (BarMar 6) than in the experiments with oblique extension (BarMar  
846 8), but due to stabilization of basins by infilling of sand, this was not documented.

847 The widening occurred mainly by fault-controlled collapse of the footwalls, and  
848 dominantly along the master faults that corresponded to the Knølegga Fault  
849 Complex, but also new intra-basin cross-faults that were initiated in the shear  
850 stage (see above) became reactivated, contributing to the complexity of the basin  
851 topography. It is not likely that a stage was reached where all (pull-apart) basin  
852 units along the margin became fully linked, although sedimentary communication  
853 along the margin may have become established.

854 During the oblique extension stage segment 1 of experiments BarMar7-9 the basin  
855 subsidence was focused in the minor pull-apart basins, which soon became linked  
856 along the regional N-S-striking basin axis. Remains of several such basin centers,  
857 of which the Sørvestsnaget Basin (Knutsen & Larsen, 1997; Kristiansen et al.,  
858 2017) is the largest, are preserved and found in seismic data (**Figure 1b**). During  
859 the experiments a continuous basin system was developed in the hanging wall  
860 side of the master fault, but it is not likely that opening occurred prior to the  
861 extension of the margin underlain by continental crust reached a stage where the  
862 separate basin units paralleling the Barents Shear Margin became linked.

863 In the subsequent inversion stage, fold populations(PSE-5-folds) with axial traces  
864 parallel to the basin axis and the master faults characterized segment 1. Remnants  
865 of such folds are locally preserved in the thickest sedimentary sequences affiliated  
866 with the Senja Shear Margin.

867

### 868 **Structures of phase 3 (contraction)**

869 The contraction (phase 3) clearly reactivated normal faults, probably causing  
870 focusing of hanging wall strain and folding, rotation of fault blocks and steepening  
871 of faults. This means that both intra-basinal and marginal faults in the Vestbakken

872 Volcanic Province can have suffered late steepening. Contraction expressed as fold  
873 systems with fold axes paralleling the basin margins development seems to  
874 correspond very well to the observed structural configuration of the Vestbakken  
875 Volcanic Province. Here pronounced tectonic inversion is focused along the N-S-  
876 striking basin margins and along some NE-SW-striking faults in the central parts  
877 of the basin. Pronounced shortening also occurred inside individual reactivated  
878 fault blocks either by bulging of the entire sedimentary sequence or as trains of  
879 folds (**Figure 12B,C**).

880

881 During phase 3 the restraining bend configuration in the northern part of segment  
882 2 was characterized by increasing contraction across strike-slip fault strands that  
883 splayed out to the northwest from the central part of segment 2 in an early stage  
884 of dextral shear. This deformation was terminated by the end of phase 1 by  
885 stacking of oblique contraction faults (PSE-5 and PSE-6-structures), defining an  
886 antiformal stack-like structure. This type of deformation falls outside the main  
887 area, but to the north this type of oblique shortening during the Eocene (phase 1)  
888 was accommodated by regional-scale strain partitioning (Leever et al., 2011a,b).

889 The Vestbakken Volcanic Province is characterized by extensive regional  
890 shortening. Onset of this event of inversion/contraction is dated to early Miocene  
891 (Jebsen & Faleide, 1998, Giennenas, 2018) and this deformation included two main  
892 structural fold styles. The first includes upright to steeply inclined closed to open  
893 anticlines that are typically present in the hanging wall of master faults. These folds  
894 typically have wavelengths in the order of 2.5 to 4.5 kilometers, and amplitudes of  
895 several hundred meters. Most commonly they appear with head-on snakehead-  
896 structures and are interpreted as buckle folds, albeit a component shear may occur in  
897 the areas of the most intense deformation, giving a snake-head-type geometry. The  
898 second style includes gentle to open anticline-syncline pairs with upright or steep to  
899 inclined axial planes open anticlines-synclines with wavelengths in the order of 5 to 7  
900 kilometers and amplitudes of several tens of meters to several hundred meters. We  
901 associate those with the PSE-4-type structures as defined in the BarMar-experiments.  
902 These folds are situated in positions where sedimentary sequences have been pushed  
903 against buttresses provided by master faults along the basin margins. The PSE-6 folds  
904 developed as fold trains in the interior basins, where buttressing against larger fault

905 walls was uncommon. Also, this pattern fits well with the development and geometry  
906 seen in the BarMar-experiments, where folding started in the central parts of the closing  
907 basins before folding of the marginal parts of the basin. In the closing stage the folding  
908 and inversion of master faults remained focused along the basin margins.

909 The experiments clearly demonstrated that contraction by buckle folding was the  
910 main shortening mechanism of the margin-parallel basin system generated in  
911 phase 2 (orthogonal or oblique extension) in all segments. In the Vestbakken  
912 Volcanic Province segments of the Knølegga Fault Complex, the EBF and the major  
913 intra-basinal faults contain clear evidence for tectonic inversion, whereas this is  
914 less pronounced in others. The hanging wall of the EBF is partly affected by fish-  
915 hook-type inversion anticlines (Ramsey & Huber, 1987; Griera et al., 2018)  
916 (**Figure 2D, E**), or isolated hanging wall anticlines or pairs or trains of synclines  
917 and anticlines (e.g.; Roberts, 1989; Coward et al., 1991; Cartwright, 1989; Mitra,  
918 1993; Uliana et al., 1995; Beauchamp et al. 1996; Gabrielsen et al. 1997; Henk &  
919 Nemcok 2008), the fold style and associated faults probably being influenced by  
920 the orientation and steepness of the pre-inversion fault (Williams et al., 1989;  
921 Cooper et al., 1989; Cooper & Warren, 2010). Some structures of this type can still  
922 be followed for many kilometers having consistent geometry and attitude. These  
923 structures have not been much modified by reactivation and are invariably found  
924 in the proximal parts footwalls of master faults, suggesting that these are  
925 inversion structures correlate to PSE-type 5-structures in the experiments  
926 developed in areas of focused contraction along pre-existing fault scarps during  
927 Oligocene inversion.

928 Trains of folds with smaller amplitudes and higher frequency are sometimes  
929 found in fault blocks in the central part of the Vestbakken Volcanic Province  
930 (**Figure 12A**). Although these structures are not dateable by seismic  
931 stratigraphical methods (on-lap configurations etc.) we regard these fold strains  
932 to be correlable with the tight folds generated in the inversion stage in the  
933 experiments (PSE-6-structures) and that they are contemporaneous with the PSE-  
934 5-structures.

935 Segment 1 in the experiments, that corresponds to the Senja Shear Margin  
936 segment, displays a structural pattern that is a hybrid between segments 1 and 2:  
937 It contains incipient structural elements that were developed in full in segments 2

938 and 3, segment 2 being dominated by releasing and restraining bend  
939 configurations and segment 3 dominated by neutral shear. Due to internal  
940 configurations, the three segments were affected to secondary (oblique) opening  
941 and contraction in various fashions. Understanding these differences was much  
942 promoted by the comparison of seismic and model data.

943

#### 944 **Some considerations about multiphase deformation in shear margins**

945 The Barents Shear Margin is a challenging target for structural analysis both  
946 because it represents a geometrically complex structural system with a multistage  
947 history, but also because high-quality (3D) reflection seismic data are limited and  
948 many structures and sedimentary systems generated in the earlier  
949 tectonothermal stages have been overprinted and obliterated by younger events.  
950 This makes analogue experiments very useful in the analysis, since they offer a  
951 template for what kind of structural elements can be expected. By constraining the  
952 experimental model according to the outline of the margin geometry and imposing  
953 a dynamic stress model in harmony according to the state-of-the-art knowledge  
954 about the regional tectono-sedimentological development, we were able to  
955 interpret the observations done in reflection seismic data in a new light.

956

957 Continental margins are commonly segmented containing primary or secondary  
958 transform elements, and pure strike-slip transforms are relatively rare (eg.  
959 Nemcok et al. 2016). Such margins, however, invariably become affected by  
960 extension following break-up and sometimes contraction due to ridge-push or far-  
961 field stress perhaps related to plate reorganization. The complexity of shear  
962 margins has ignited several conceptual discussions. One such discussion concerns  
963 the presence of zones of weakness prior to break-up (eg. Sibuet & Mascle 1978;  
964 Taylor et al, 2009; Gibson et al. 2013; Basile 2015). In the case of the Barents Shear  
965 Margin the de Geer zone provides such a pre-existing zone of weakness, and this  
966 premise was acknowledged when the scaled model was established. The  
967 relevance of our model is therefore constrained to cases where a crustal-scale  
968 zone of weakness existed before break-up. Furthermore, in cases with pre-  
969 existing zones of weakness, our model demonstrates that the inipient architecture

970 of the margin is important indeed and the detailed geometry and width of the pre-  
971 existing weak zone must be mapped and included in the model.

972

## 973 **Summary and conclusions**

974

975 Our observations confirmed that the main segments of the Barents Shear Margin,  
976 albeit undergoing the same regional stress regime, display contrasting structural  
977 configurations

978

979 The deformation in segment 2 in the BarMar-experiments, was determined by  
980 releasing and restraining bends in the southern and northern parts, respectively.  
981 Thus, the southern part, corresponding to the Vestbakken Volcanic Province, was  
982 dominated by the development of a regional-scale extensional shear duplex as  
983 defined by Woodcock & Fischer (1983) and Twiss & Moores (2007). By continued  
984 shear the basin developed into a full-fledged pull-apart basin or rhomb graben  
985 (Crowell, 1974; Aydin & Nur, 1982) in which rotating fault blocks were trapped.  
986 The pull-apart-basin became the nucleus for greater basin systems to develop in  
987 the following phase of extension also providing the space for folds to develop in  
988 the contractional phase.

989

990 We conclude that fault- and fold systems found in the realm of the Vestbakken  
991 Volcanic Province are in accordance with a three-stage development that includes  
992 dextral shear followed by oblique extension and contraction ( $315/135^0$ ) along a  
993 shear margin with composite geometry.

994 Folds with NE-SW-trending fold axes that are dominant in wider area of the  
995 Vestbakken Volcanic Province and are dominated by folds in the hanging walls of  
996 (older) normal faults, sometimes characterized by narrow, snake-head- or  
997 harpoon-type structures that are typical for tectonic inversion (Cooper et al.,  
998 1989; Coward, 1994; Allmendinger, 1998; Yameda & McClay, 2004; Pace &  
999 Calamitra, 2014) typical of inverted faults.

1000

1001 Comparing seismic mapping and analogue experiments it is evident that a main  
1002 challenge in analyzing the structural pattern in shear margins of complex

1003 geometry and multiple reactivation is the low potential for preservation of  
1004 structures that were generated in the earliest stages of the development.

1005

1006

1007

1008

1009

1010

1011

1012

1013

1014

1015

1016

1017

1018

1019

1020

1021

1022

1023

1024

1025

1026

1027

1028

1029

1030

1031

1032

1033

1034

1035

1036 **Author contribution**

1037 R.H.Gabrielsen: Contributions to outline, design and performance of experiments.

1038 First writing and revisions of manuscript. First drafts of figures.

1039 P.A.Giennenas: Seismic interpretation in the Vestbakken Volcanic Province.

1040 Identification and description of fold families.

1041 Suggestion:

1042 D.Sokoutis: Main responsibility for set-up, performance and handling of  
1043 experiments. Revisions of manuscript.

1044 E.Willigshofer: Performance and handling of experiments. Revisions of  
1045 manuscript. Design and revisions of figure material.

1046 M. Hassaan: Background seismic interpretation. Discussions and revisions of  
1047 manuscript. Design and revisions of figure material.

1048 J.I.Faleide: Regional interpretations and design of experiments. Participation in  
1049 performance and interpretations of experiments. Revisions of manuscript, design  
1050 and revisions of figure material.

1051

1052 **Acknowledgements**

1053 The work was supported by ARCEX (Research Centre for Arctic Petroleum  
1054 Exploration), which was funded by the Research Council of Norway (grant number  
1055 228107) together with 10 academic and six industry (Equinor, Vår Energi, Aker  
1056 BP, Lundin Energy Norway, OMV and Wintershall Dea) partners. Muhammad  
1057 Hassaan was funded by the Suprabasins project (Research Council of Norway  
1058 grant no. 295208). We thank to Schlumberger for providing us with academic  
1059 licenses for Petrel software to do seismic interpretation. Two anonymous  
1060 reviewers and the editors of this special volume provided comments, suggestions  
1061 and advice that enhanced the clarity and scientific quality of the paper.

1062

1063



1064 **References**

1065

1066 Allemand P. and Brun J.P.: Width of continental rifts and rheological layering of the  
1067 lithosphere. *Tectonophysics*, 188, 63-69, 1991.

1068 Allmendinger, R.W.: : Inverse and forward numerical modeling of three shear  
1069 fault-propagation folds, *Tectonics*, 17(4), 640-656, 1998.

1070 Auzemery, A., E. Willingshofer, D. Sokoutis, J.P. Brun and Cloetingh S.A.P.L.,:  
1071 Passive margin inversion controlled by stability of the mantle lithosphere,  
1072 *Tectonophysics*, 817, 229042, 1-17,  
1073 <https://doi.org/10.1016/j.tecto.2021.229042>, 2021.

1074 Aydin,A. and Nur,A.:1982: Evolution of pull-apart basins and their scale  
1075 independence. *Tectonics*, 1, 91-105, 1982.

1076

1077 Ballard J-F., Brun J-P. and Van Ven Driessche J.: Propagation des chevauchements  
1078 au-dessus des zones de décollement: modèles expérimentaux. *Comptes Rendus de*  
1079 *l'Académie des Sciences, Paris*, 11, 305, 1249-1253, 1987.

1080

1081 Basile, C.: Transform continental margins – Part 1: Concepts and models.  
1082 *Tectonophysics*, 661, pp.1-10. doi: 10.1016/j.tecto.2015.08.034, 2015.

1083

1084 Basile,C. and Brun,J.-P.: Transtensional faulting patterns ranging from pull-apart  
1085 basins to transform continental margins: an experimental investigation, *Journal of*  
1086 *Structural Geology*, 21,23-37, 1997.

1087

1088 Beauchamp,W., Barazangi,M., Demnati,A. and El Alji,M.: Intracontinental rifting  
1089 and inversion: Missouri Basin and Atlas Mountains, Morocco. *American*  
1090 *Association of Petroleum Geologists Bulletin*, 80(9), 1455-1482, 1996.

1091

1092 Bergh,S.G., Braathen,A. and Andresen,A.: Interaction of basement-involved and  
1093 thin-skinned tectonism in the Tertiary fold-and-thrust belt of Central Spitsbergen,  
1094 Svalbard. *American Association of Petroleum Geologists Bulletin*, 81(4), 637-  
1095 661,1997.

1096

1097 Bergh,S.G. and Grogan,P.: Tertiary structure of the Sørkapp-Hornsund Region,  
1098 South Spitsbergen, and implications for the offshore southern extension of the  
1099 fold-thrust-belt. *Norwegian Journal of Geology*, 83, 43-60, 2003.

1100

1101 Biddle, K.T. and Christie-Blick, N., (eds.): Strike-Slip Deformation, Basin  
1102 Formation, and Sedimentation: Society of Economic Paleontologists and  
1103 Mineralogists Special Publication, 37, 386pp, 1985a.

1104

1105 Biddle, K.T. and Christie-Blick, N.: Glossary — Strike-slip deformation, basin  
1106 formation, and sedimentation, *in*: Biddle, K.T., and Christie-Blick, N. (eds.): Strike-  
1107 Slip Deformation, Basin Formation, and Sedimentation: Society of Economic  
1108 Paleontologists and Mineralogists Special Publication, 37, 375-386, 1985b

1109

1110 Blaich,O.A., Tsikalas,F. and Faleide,J.I.: New insights into the tectono-stratigraphic

1111 evolution of the southern Stappen High and the transition to Bjørnøya Basin, SW  
1112 Barents Sea, Marine and Petroleum Geology, 85, 89-105, doi:  
1113 10.1016/j.marpetgeo.2017.04.015, 2017.  
1114  
1115 Breivik,A.J., Faleide,J.I. and Gudlaugsson,S.T.: Southwestern Barents Sea margin:  
1116 late Mesozoic sedimentary basins and crustal extension, Tectonophysics, 293, 21-  
1117 44, 1998.  
1118  
1119 Breivik,A.J., Mjelde,R., Grogan,P., Shinamura,H., Murai,Y. and Nishimura,Y.: Crustal  
1120 structure and transform margin development south of Svalbard based on ocean  
1121 bottom seismometer data. Tectonophysics, 369, 37-70 2003.

1122 Brekke, H.: The tectonic evolution of the Norwegian Sea continen- tal margin with  
1123 emphasis on the Vøring and Møre basins: Geological Society, London, Special  
1124 Publication, 136, 327-378, 2000.

1125 Brekke, H. and Riis, F.: Mesozoic tectonics and basin evolution of the Norwegian  
1126 Shelf between 60°N and 72°N. Norsk Geologisk Tidsskrift, 67, 295-322, 1987.  
1127  
1128 Burchfiel, B.C. and Stewart,J.H.: "Pull-apart" origin of the central segment of Death  
1129 Valley, California. Geological Society of America Bulletin, 77, 439-442, 1966.  
1130  
1131 Campbell,J.D.: *En échelon* folding, Economical Geology, 53(4), 448-472, 1958.  
1132  
1133 Cartwright,J.A.: The kinematics of inversion in the Danish Central Graben. in:  
1134 M.A.Cooper & G.D.Williams (eds.): Inversion Tectonics. Geological Society of  
1135 London Special Publication, 44, 153-175, 1989.  
1136  
1137 Casas, A.M., Gapals,D., Nalpas,T., Besnard,K. and Román-Berdiel,T.: Analogue  
1138 models of transpressive systems, Jornal of Structural Geology, 23,733-743, 2001  
1139  
1140 Christie-Blick,N. and Biddle,K.T.: Deformation and basin formation along strike-  
1141 slip faults. in: Biddle,K.T. & Christie-Blick,N. (eds.): Strike-slip deformation, basin  
1142 formation and sedimentation. Society of Economic Mineralogists and  
1143 Palaeontologists (Tulsa Oklahoma), Special Publication, 37, 1-34, 1985.  
1144  
1145 Cloos,H.: Experimenten zur inneren Tectonick, Zentralblatt für Mineralogie,  
1146 Geologie und Palaentologie, 1928B, 609-621, 1928.  
1147  
1148 Cloos,H.: Experimental analysis of fracture patterns, Geological Society of America  
1149 Bulletin, 66(3), 241-256, 1955.  
1150  
1151 Cooper,M. and Warren,M.J.: The geometric characteristics, genesis and petroleum  
1152 significance of inversion structures, in Law,R.D., Butler,R.W.H., Holdsworth,R.E.,  
1153 Krabbendam,M. & Strachan,R.A. (eds.): Continental Tectonics and Mountain  
1154 Building: The Lagacy of Peache and Horne, Geological Society of London, Special  
1155 Publication, 335, 827-846, 2010.  
1156  
1157 Cooper,M.A., Williams,G.D., de Graciansky,P.C., Murphy,R.W., Needham,T., de

1158 Paor,D., Stoneley,R., Todd,S.P., Turner,J.P. and Ziegler,P.A.: Inversion tectonics – a  
1159 discussion. Geological Society, London, Special Publications, 44, 335-347, 1989.  
1160  
1161 Coward, M.: Inversion tectonics, in: Hancock,P.L. (ed.): Continental Deformation,  
1162 Pergamon Press, 289-304, 1994.  
1163  
1164 Coward, M.P., Gillcrist, R. and Trudgill, B.: Extensional structures and their tectonic  
1165 inversion in the Western Alps, *in*: A.M.Roberts, G.Yielding & B.Freeman (eds.): The  
1166 Geometry of Normal Faults. Geological Society of London Special Publication, 56,  
1167 93-112 1991.  
1168  
1169 Crowell, J.C.: Displacement along the San Andreas Fault, California, Geological  
1170 Society of America Special Papers, 71, 59pp, 1962.  
1171  
1172 Crowell, J.C.: Origin of late Cenozoic basins in southern California. in Dorr, R.H. and  
1173 Shaver, R.H. (eds.): Modern and ancient geosynclinal sedimentation. SEPM Special  
1174 Publication, 19, 292-303, 1974a  
1175  
1176 Crowell, J.C., 1974b: Implications of crustal stretching and shortening of coastal  
1177 Ventura Basin, *in*: Howell,D.G. (ed.): Aspects of the geological history of the  
1178 California continental Borderland, American Association of Petroleum Geologists,  
1179 Pacific Section,Publication, 24, 365-382, 1974b  
1180  
1181 Cunningham, W.D. and Mann, P. (eds.): : Tectonics of Strike-Slip Restraining and  
1182 Releasing Bends, Geological Society London Special Publication, 290, 482pp,  
1183 2007a.  
1184  
1185 Cunningham, W.D. and Mann, P.: Tectonics of Strike-Slip Restraining and  
1186 Releasing Bends, *in*: Cunningham,W.D. & Mann,P. (eds.), 2007: Tectonics of Strike-  
1187 Slip Restraining and Releasing Bends, Geological Society London Special  
1188 Publication, 290, 1-12, 2007b.  
1189  
1190 Dauteuil, O. and Mart, Y.: Analogue modeling of faulting pattern, ductile  
1191 deformation, and vertical motion in strike-slip fault zones, *Tectonics*, 17(2), 303-  
1192 310, 1998.  
1193  
1194 Del Ventisette, C., Montanari, D., Sani, F., Bonini, M. and Corti, G.: Reply to comment  
1195 by J. Wickham on “Basin inversion and fault reactivation in laboratory  
1196 experiments”. *Journal of Structural Geology* 29, 1417–1418, 2007.  
1197  
1198 Dooley, T. and McClay, K.: Analog modeling of pull-apart basins, *American*  
1199 *Association of Petroleum Geologists Bulletin*, 81(11), 1804-1826, 1997.  
1200  
1201 Dooley, T.P. and Schreurs, G.:Analogue modelling of intraplate strike-slip  
1202 tectonics: A review and new experimental results, *Tectonophysics*, 574-575, 1-71,  
1203 2012  
1204

1205 Doré, A.G. and Lundin, E.R.: Cenozoic compressional structures on the NE Atlantic  
1206 margin: nature, origin and potential significance for hydrocarbon exploration.  
1207 Petroleum Geosciences, 2, 299-311, 1996  
1208

1209 Doré, A.G., Lundin, E.R., Gibbons, A., Sømme, T.O. and Tørudbakken, B.O.:  
1210 Transform margins of the Arctic: a synthesis and re-evaluation *in*: Nemcok,M.,  
1211 Rybár,S., Sinha,S.T., Hermeston,S.A. & Ledvényiová,L. (eds.): Transform Margins:;  
1212 Development, Control and Petroleum Systems, Geological Society London, Special  
1213 Publication, 431, 63-94, 2016.  
1214

1215 Doré, A.G., Lundin, E.R., Jensen, L.N., Birkeland, Ø., Eliassen, P.E. and Fichler, C.:  
1216 Principal tectonic events in the evolution of the northwest European Atlantic  
1217 margin. In: A.J.Fleet & S.A.R.Boldy (eds.): Petroleum Geology of Northwest Europe:  
1218 Proceedings of the Fifth Conference (Geological Society of London), 41-61, 1999.  
1219

1220 Eidvin, T., Goll, R.M., Grogan, P., Smelror, M. and Ulleberg, K.: The Pleistocene to  
1221 Middle Eocene stratigraphy and geological evolution of the western Barents Sea  
1222 continental margin ta well site 731675-1 (Bjørnøya West area). Norsk Geologisk  
1223 Tidsskrift, 78, 99-123 1988.  
1224

1225 Eidvin, T., Jansen, E. and Riis,F.: Chronology of Tertiary fan deposits off the  
1226 western Barents Sea: Implications for the uplift and erosion history of the Barents  
1227 Shelf. Marine Geology, 112, 109-131, 1993.  
1228

1229 Eldholm, O., Faleide, J.I. and Myhre, A.M.: Continent-ocean transition at the  
1230 western Barents Sea/Svalbard continental margin. Geology, 15, 1118-1122, 1987.  
1231

1232 Eldholm, O., Thiede, J., and Taylor, E.: Evolution of the Vøring volcanic margin, *in*:  
1233 Eldholm, O., Thiede, J., and Taylor, E., (eds.): Proceedings of the Ocean Drilling  
1234 Program, Scientific Results, 104: College Station (Ocean Drilling Program), TX,  
1235 1033-1065, 1989.  
1236

1237 Eldholm, O., Tsikalas, F. and Faleide,J.I.: Continental margin off Norway 62-  
1238 75°N:Paleogene tectono-magmatic segmentation and sedimentation. Geological  
1239 Society of London Special Publication, 197, 39-68, 2002  
1240

1241 Emmons, R.C.: Strike-slip rupture patterns in sand models, Tectonophysics, 7, 71-  
1242 87, 1969.  
1243

1244 Faugère, E., Brun, J.-P. and Van Den Driessche, J.: Bassins asymétriques en  
1245 extension pure et en détachements:Modèles expérimentaux, Bulletin Centre  
1246 Recherche Exploration et Production Elf Aquitaine, 10(2), 13-21, 1986.  
1247

1248 Faleide, J.I., Bjørlykke, K. and Gabrielsen, R.H.: Geology of the Norwegian Shelf. *in*:  
1249 Bjørlykke,K.: Petroleum Geoscience: From Sedimentary Environments to Rock  
1250 Physics 2<sup>nd</sup> Edition, Springer-Verlag, Berlin Heidelberg, Chapter 25, 603 -637,  
1251 2015.  
1252

1253 Faleide, J.I., Myhre, A.M. and Eldholm, O.: Early Tertiary volcanism at the western

1254 Barents Sea margin. in: A.C.Morton & L.M.Parsons (eds.): Early Tertiary volcanism  
1255 and the opening of the NE Atlantic.Geological Society of London Special  
1256 Publication, 39,135-146, 1988.  
1257

1258 Faleide, J.I., Tsikalas, F., Breivik, A.J, Mjelde, R., Ritzmann, O., Engen, Ø., Wilson, J.  
1259 and Eldholm, O.: Structure and evolution of the continental margin off Norway and  
1260 the Barents Sea. Episodes, 31(1), 82-91, 2008.  
1261

1262 Faleide, J.I., Vågnes, E. and Gudlaugsson, S.T.: Late Mesozoic - Cenozoic evolution  
1263 of the south-western Barents Sea in a regional rift-shear tectonic setting. Marine  
1264 and Petroleum Geology, 10, 186-214, 1993  
1265

1266 Fichler, C. and Pastore, Z.: Petrology and crystalline crust in the southwestern  
1267 Barents Sea inferred from geophysical data. Norwegian Journal of Geology, 102,  
1268 41pp, <https://dx.doi.org/10.17850/njg102-2-2>, 2022.  
1269

1270 Freund, R.: The Hope Fault, a strike-slip fault in New Zealand, New Zealand  
1271 Geological Survey Bulletin, 86, 1-49, 1971.  
1272

1273 Gabrielsen, R.H.: Structural elements in graben systems and their influence on  
1274 hydrocarbon trap types. in: A.M. Spencer (ed.): Habitat of Hydrocarbons on the  
1275 Norwegian Continental Shelf. Norw. Petrol. Soc. (Graham & Trotman), 55 – 60,  
1276 1986.  
1277

1278 Gabrielsen, R.H., Færseth, R.B., Jensen, L.N., Kalheim, J.E. and Riis, F.: Structural  
1279 elements of the Norwegian Continental Shelf. Part I: The Barents Sea Region.  
1280 Norwegian Petroleum Directorate, Bulletin, 6, 33pp, 1990.  
1281

1282 Gabrielsen, R.H., Grunnaleite, I. and Rasmussen, E.: Cretaceous and Tertiary  
1283 inversion in the Bjørnøyrenna Fault Complex, south-western Barents Sea. Marine  
1284 and Petroleum Geology, 142, 165-178, 1997.  
1285

1286 Gac, S., Klitzke, P., Minakov, A., Faleide, J.I. and Scheck-Wenderoth, M.:  
1287 Lithospheric strength and elastic thickness of the Barents Sea and Kara Sea  
1288 region, Tectonophysics, 691, 120-132, doi: 10.106/j.tecto.2016.04.028, 2016.  
1289

1290 Gaina, C., Gernigon, L. and Ball.P.: Palaeocene – Recent plate boundaries in the NE  
1291 Atlantic and the formation of the Jan Mayen microcontinent. Journal of the  
1292 Geological Society, London, 166(4), 601-616, 2009.

1293 Ganerød, M., Smethurst, M.A., Torsvik, T.H., Prestvik, T., Rouse, S., McKenna, C.,  
1294 van Hinsbergen, D.J.J. and Hendriks, W.W.H.: The North Atlantic Igneous Province  
1295 reconstructed and its relation to the Plume Generation Zone: the Antrim Lava  
1296 Group revisited. Geophysical Journal International, 182, 183-202, doi:  
1297 10.1111/j.1365-246X.2010.04620.x, 2010.

1298 Gibson, G.M., Totterdell, J.M., White, N. Mitchell, C.H., Stacey, A.R., M. P. Morse,  
1299 M.P. and A. Whitaker: Preexisting basement structures and its influence on  
1300 continental rifting and fracture development along Australia's southern rifted

1301 margin, *Journal of the Geological Society of London*, 170, 365-377, 2013.

1302 Giennenas, P.A.: The Structural development of the Vestbakken Volcanic Province,  
1303 Western Barents Sea. Relation between Ffaults and folds, Unpubl. Master thesis,  
1304 University of Oslo 2018, 89 pp, 2018.

1305

1306 Graymer, R.W., Langenheim, V.E., Simpson, R.W., Jachens, R.C. and Ponce, D.A.:  
1307 Relative simple through-going fault planes at large-earthquake depth may be  
1308 concealed by surface complexity of strike-slip faults, *in*: Cunningham,W.D. &  
1309 Mann,P. (eds.): *Tectonics of Strike-Slip Restraining and Releasing Bends*,  
1310 Geological Society London Special Publication, 290, 189-201, 2007.

1311

1312 Griera, A., Gomez.Rivas, E. and Llorens,M.-G.: The influence of layer-interface  
1313 geometry of single-layer folding. *Geological Society of London Special Publication*  
1314 487, SP487:4, 2018.

1315

1316 Grogan, P., Østvedt-Ghazi, A.-M., Larssen, G.B., Fotland, B., Nyberg, K., Dahlgren, S.  
1317 and Eidvin, T.: Structural elements and petroleum geology of the Norwegian sector  
1318 of the northern Barents sea. *in*: Fleet,A.J. & Boldry,S.A.R. (eds.): *Petroleum Geology*  
1319 *of Northwest Europe: Proceedings of the 5th Conference*, Geological Society of  
1320 London, 247-259, 1999.

1321

1322 Groshong, R.H.: Half-graben structures: balanced models of extensional fault bend  
1323 folds, *Geological Society of America Bulletin*, 101, 96-195, 1989

1324

1325 Gudlaugsson, S.T. and Faleide, J.I.: The continental margin between Spitsbergen &  
1326 Bjørnøya, *in*: O.Eiken (ed.): *Seismic Atlas of Western Svalbard*, Norsk Polarinstutt  
1327 Meddelelser, 130, 11-13, 1994.

1328

1329 Gudlaugsson, S.T., Faleide, J.I., Johansen, S.E. and Breivik, A.J.: Late Palaeozoic  
1330 structural development of the south-western Barents Sea. *Marine and Petroleum*  
1331 *Geology*, 15, 73-102, 1998.

1332

1333 Hamblin, W.K.: Origin of "reverse drag" on the down-thrown side of normal faults,  
1334 *Geological Society of America Bulletin*, 76, 1145-1164., 1965.

1335

1336 Hanisch, J.: The Cretaceous opening of the Northeast Atlantic. *Tectonophysics*,  
1337 101, 1-23, 1984.

1338

1339 Harding, T.P.: Petroleum traps associated with wrench faults. *American*  
1340 *Association of Petroleum Geologists Bulletin*, 58, 1290-1304, 1974.

1341

1342 Harding, T.P. and Lowell, J.D.: Structural styles, their plate tectonic habitats, and  
1343 hydrocarbon traps in petroleum provinces, *American Association of Petroleum*  
1344 *Geologists Bulletin*, 63,1016-1058, 1979.

1345

1346 Harland, W.B.: The tectonic evolution of the Arctic-North Atlantic Region, *in*:  
1347 Taylor,J.H., Rutten,M.G., Hales,A.L., Shackelton,R.M., Nairn,A.E. & Harland:W.B.:  
1348 Discussion, *A Symposium on Continental Drift*, *Philosophical Transactions of the*  
1349 *Royal Society of London*,, Series A, 258, 1088, 59-75, 1965.

- 1350  
1351 Harland, W.B.: Contributions of Spitsbergen to understanding of tectonic  
1352 evolution of North Atlantic Region, American Association of Petroleum Geologists,  
1353 Memoir 12, 817-851, 1969.  
1354  
1355 Harland, W.B.: Tectonic transpression in Caledonian Spitsbergen, Geological  
1356 Magazine, 108, 27-42, 1971  
1357  
1358 Henk, A. and Nemcok, M.: Stress and fracture prediction in inverted half-graben  
1359 structures. Journal of Structural Geology, 30(1), 81-97, 2008.
- 1360 Horni, J.Á., Hopper, J.R., Blischke, A., Geisler, W.H., Stewart, M., Mcdermott, K.,  
1361 Judge, M., Erlendsson, Ö. and Ártíng, U.E.: Regional Distribution of Volcanism  
1362 within the North Atlantic Igneous Province. The NE Atlantic Region: A Reappraisal  
1363 of Crustal Structure, Tectonostratigraphy and Magmatic Evolution. Geological  
1364 Society, London, Special Publications, 447, 105-125,  
1365 <https://doi.org/10.1144/SP447.18>, 2017.
- 1366 Horsfield, W.T., 1977: An experimental approach to basement-controlled faulting.  
1367 Geologie en Mijbouw, 56(4), 3634-370 1977.  
1368  
1369 Hubbert, M.K.: Theory of scale models as applied to the study of geologic  
1370 structures, Bulletin Geological Society of America, 48, 1459-1520, 1937.
- 1371 Jebesen, C. and Faleide, J.I.: Tertiary rifting and magmatism at the western Barents  
1372 Sea margin (Vestbakken volcanic province). III international conference on Arctic  
1373 margins, ICAM III; abstracts; plenary lectures, talks and posters, 92, 1998.
- 1374 Khalil,S.M. and McClay,K.R.: 3D geometry and kinematic evolution of extensional  
1375 fault-related folds, NW Red Sea, Egypt. in: Childs,C., Holdswort,R.E., Jackson,C.A.L.,  
1376 Manzocchi,T., Walsh,J.J & Yielding,G. (eds.): The Geometry and Growth of Normal  
1377 Faults, Geological Society, London, Special Publication 439,  
1378 doi.org/10.1144/SP439.11, 2016.  
1379  
1380 Klinkmüller, M., Schreurs, G., Rosenau, M. and Kemnitz, H.: Properties of  
1381 granular analogue model materials: a community wide survey. Tectonophysics  
1382 684, 23-38. <http://dx.doi.org/10.1016/j.tecto.2016.01.017.feb.>, 2016.  
1383  
1384 Knutsen, S.-M. and Larsen,K.I.: The late Mesozoic and Cenozoic evolution of the  
1385 Sørvestsnaget Basin: A tectonostratigraphic mirror for regional events along the  
1386 Southwestern Barents Sea Margin? Marine and Petroleum Geology, 14(1), 27-54,  
1387 1997.  
1388  
1389 Kristensen, T.B., Rotevatn, A., Marvik, M., Henstra, G.A., Gawthorpe, R.L. and  
1390 Ravnås, R.: Structural evolution of sheared basin margins: the role of strain  
1391 partitioning. Sørvestsnaget Basin, Norwegian Barents Sea, Basin Research, (2017),  
1392 1-23, doi:10.1111/bre.12235, 2017.  
1393  
1394 Le Calvez, J-H. and Vendeville, : Experimental designs to mode along strike-slip

- 1395 fault interaction. *in*: Scellart, W.P. & Passcheir, C. (eds.). Analogue Modeling of  
1396 large-scale Tectonic Processes, Journal of Virtual Explorer, 7, 7-23, 2002.  
1397
- 1398 Leever, K.A., Gabrielsen, R.H., Sokoutis, D. and Willingshofer, E.: The effect of  
1399 convergence angle on the kinematic evolution of strain partitioning in  
1400 transpressional brittle wedges: insight from analog modeling and high resolution  
1401 digital image analysis. Tectonics, 30, TC2013, 1-25, doi: 10.1029/2009TC002649,  
1402 2011a.  
1403
- 1404 Leever, K.A., Gabrielsen, R.H., Faleide, J.I. and Braathen, A.: A transpressional  
1405 origin for the West Spitsbergen Fold and Thrust Belt - insight from analog  
1406 modeling. Tectonics, 30, TC2014, 1- 24, doi: 10.1029/2010TC002753, 2011b.  
1407
- 1408 Libak, A., Mjelde, R., Keers, H., Faleide, J.I. and Murai, Y.: An integrated geophysical  
1409 study of Vestbakken Volcanic Province, western Barents Sea continental margin,  
1410 and adjacent oceanic crust, Marine Geophysical Research, 33(2), 187-207, 2012.  
1411
- 1412 Lorenzo, J.M.: Sheared continental margins: an overview, Geo-Marine Letters,  
1413 17(1), 1-3, 1997
- 1414 Lowell, J.D., 1972: Spitsbergen Tertiary orogenic belt and the Spitsbergen fracture  
1415 zone, Geol. Soc. Am. Bull., 83, 3091–3102, doi:10.1130/0016-  
1416 7606(1972)83[3091:STOBAT]2.0.CO;2, 1972.
- 1417 Lundin, E.R. and Doré, A.G.: A tectonic model for the Norwegian passive margin  
1418 with implications for the NE Atlantic.: Early Cretaceous to break-up. Journal of the  
1419 Geological Society London, 154, 545-550, 1997.  
1420
- 1421 Lundin, E.R., Doré, A.G., Rønning, K. and Kyrkjebø, R.: Repeated inversion in the  
1422 Late Cretaceous-Cenozoic northern Vøring Basin, offshore Norway, Petroleum  
1423 Geoscience, 19(4), 329-341, 2013.  
1424
- 1425 Luth, S., Willingshofer, E., Sokoutis, D. and Cloetingh, S.: analogue modelling of  
1426 continental collision: Influence of plate coupling on mantle lithosphere subduction,  
1427 crustal deformation and surface topography, Tectonophysics, 4184, 87-102, doi:  
1428 10.1016/j.tecto2009.08.043, 2010.
- 1429 Maher, H. D., Jr., Bergh, S., Braathen, A. and Ohta, Y.: Svartfjella, Eidembukta, and  
1430 Daudmannsodden lineament: Tertiary orogen-parallel motion in the crystalline  
1431 hinterland of Spitsbergen's fold-thrust belt, Tectonics, 16(1), 88–106,  
1432 doi:10.1029/96TC02616, 1997.
- 1433 Mandl, G., de Jong, L.N.J. and Maltha, A.: Shear zones in granular material. Rock  
1434 Mechanics, 9, 95–144, 1977.  
1435
- 1436 Manduit, T. and Dauteuil, O.: Small scale modeling of oceanic transform zones,  
1437 Journal of Geophysical Research, 101(B9), 20195-20209, 1996.  
1438
- 1439 Mann, P.: Global catalogue, classification and tectonic origins of restraining and



1440 releasing bends on active and ancient strike-slip fault systems. *in*: Cunningham,  
1441 W.D. and Mann,P. (eds.), 2007: Tectonics of Strike-Slip Restraining and Releasing  
1442 Bends, Geological Society London Special Publication, 290, 13-142, 2007.  
1443  
1444 Mann, P., Hempton, M.R., Bradley, D.C. and Burke,K.: Development of pull-apart  
1445 basins. *Journal of Geology*, 91(5), 529-554, 1983.  
1446  
1447 Mascle, J. & Blarez, E.: Evidence for transform margin evolution from the Ivory  
1448 Coast Ghana continental margin, *Nature*, 326, 378-381, 1987.  
1449  
1450 McClay. K.R., 1990: Extensional fault systems in sedimentary basins. A review of  
1451 analogue model studies, *Marine and Petroleum Geology*, 7, 206-233, 1990.  
1452  
1453 Mitra, S.: Geometry and kinematic evolution of inversion structures. *American*  
1454 *Association of Petroleum Geologists Bulletin*, 77, 1159-1191, 1993.  
1455  
1456 Mitra, S. and Paul, D.: Structural geology and evolution of releasing and  
1457 constratrining bends: Insights from laser-scanned experimental models,  
1458 *American Association of Petroleum Geologists Bulletin*, 95(7), 1147-1180, 2011.  
1459  
1460 Morgenstern, N.R. and Tchalenko, J.S.: Microscopic structures in kaolin subjected  
1461 to direct shear, *Géotechnique*, 17, 309-328, 1967.  
1462  
1463 Mosar, J., Torsvik, T.H. & the BAT Team: Opening of the Norwegian and Greenland  
1464 Seas: Plate tectonics in mid Norway since the late Permian. in: E.Eide (ed.):  
1465 BATLAS. Mid Norwegian plate reconstruction atlas with global and Atlantic  
1466 perspectives. Geological Survey of Norway, 48-59, 2002.  
1467  
1468 Mouslopoulou, V., Nicol, A., Little, T.A. and Walsh,J.J.: Terminations of large-strike-  
1469 slip faults: an alternative model from New Zealand, in: Cunningham, W.D. and  
1470 Mann, P. (eds.): Tectonics of Strike-Slip Restraining and Releasing Bends,  
1471 Geological Society London Special Publication, 290, 387- 415, 2007.  
1472  
1473 Mouslopoulou, V., Nicol, A., Walsh, J.J., Beetham, D. and Stagpoole, V.: Quaternary  
1474 temporal stability of a regional strike-slip and rift fault interaction. *Journal of*  
1475 *Structural Geology*, 30, 451-463, 2008.  
1476  
1477 Myhre, A.M. and Eldholm, O.: The western Svalbard margin (74-80°N). *Marine and*  
1478 *Petroleum Geology*, 5, 134-156, 1988.  
1479  
1480 Myhre, A.M., Eldholm, O. and Sundvor, E.: The margin between Senja and  
1481 Spitsbergen Fracture Zones: Implications from plate tectonics. *Tectonophysics*,  
1482 89, 33-50, 1982.  
1483  
1484 Naylor, M.A., Mandl, G and Sijpestijn, C.H.K.: Fault geometries in basement-induced  
1485 wrench faulting under different initial stress states. *Journal of Structural Geology*,  
1486 8, 737-752, 1986.  
1487

1488 Nemcok, M., Rybár, S., Sinha, S.T., Hermeston, S.A. and Ledvényiová, L.: Transform  
1489 margins: development, controls and petroleum systems – an introduction. *in*:  
1490 Nemcok, M., Rybár, S., Sinha, S.T., Hermeston, S.A. and Ledvényiová, L. (eds.):  
1491 Transform Margins: Development, Control and Petroleum Systems, Geological  
1492 Society London, Special Publication, 431, 1-38, 2016.  
1493

1494 Odone, F. and Vialon, P.: Analogue models of folds above a wrench fault,  
1495 Tectonophysics, 990,31-46, 1983  
1496

1497 Pace, P. and Calamita, F.: Push-up inversion structures v. fault-bend reactivation  
1498 anticlines along oblique thrust ramps: examples from the Apennines fold-and-  
1499 thrust-belt, Italy, Journal Geological Society London, 171, 227-238, 2014.  
1500

1501 Pascal, C. and Gabrielsen, R.H.: Numerical modelling of Cenozoic stress patterns in  
1502 the mid Norwegian Margin and the northern North Sea. Tectonics, 20(4), 585-599,  
1503 2001.  
1504

1505 Pascal, C., Roberts, D. and Gabrielsen, R.H.: Quantification of neotectonic stress  
1506 orientations and magnitudes from field observations in Finnmark, northern  
1507 Norway. Journal of Structural Geology, 27, 859-870, 2005.  
1508

1509 Peacock, D.C.P., Nixon, C.W., Rotevatn, A., Sanderson, D.J. and Zuluaga, L.F.:  
1510 Glossary of fault and other fracture networks, Journal of Structural Geology, 92,  
1511 12-29, doi: 10.1016/j.jgs2016.09.008, 2016.  
1512

1513 Perez-Garcia, C., Safranová, P.A., Mienert, J., Berndt, C. and Andreassen, K.:  
1514 Extensional rise and fall of a salt diapir in the Sørvestsnaget Basin, SW Barents Sea.  
1515 Marine and Petroleum Geology, 46, 129-134, 2013.  
1516

1517 Planke, S., Alvestad, E. and Eldholm, O.: Seismic characteristics of  
1518 basaltic extrusive and intrusive rocks: The Leading Edge, 18(3), 342-348.  
1519 <https://doi-org.ezproxy.uio.no/10.1190/1.1438289>, 1999.  
1520

1521 Ramberg, H.: Gravity, deformation and the Earth's crust, Academic Press, New  
1522 York, 214pp, 1967.  
1523

1524 Ramberg, H.: Gravity, deformation and the Earth's crust, 2nd edition. Academic  
1525 Press, New York 452pp, 1981  
1526

1527 Ramsay, J.G. and Huber, M.I., 1987: The techniques of modern structural geology.  
1528 Vol. 2: Folds and fractures. Academic Press, London, 309-700, 1987.  
1529

1530 Reemst, P., Cloetingh, S. and Fanavoll, S.: Tectonostratigraphic modelling of  
1531 Cenozoic uplift and erosion in the south-western Barents Sea. Marine and  
1532 Petroleum Geology, 11, 478-490, 1994.  
1533

1534 Richard, P.D., Ballard, B., Colletta, B. and Cobbold, P.R.: Naissance et evolution de  
1535 failles au dessus d'un décrochement de socle: Modélisation experimental et  
1536 tomographie, C. R. Acad.Sci. Paris, 308,9, 2111-2118, 1989.

- 1537  
1538 Richard, P.D. and Cobbold, P.R.: Structures et fleur positives et décrochements  
1539 crustaux: modélisation analogique et interpretation mecanique,  
1540 C.R.Acad.Sci.Paris, 308, 553-560, 1989.
- 1541  
1542 Richard, P. and Krantz, R.W.: Experiments on fault reactivation in strike-slip mode,  
1543 Tectonophysics, 188, 117-131, 1991.
- 1544  
1545 Richard, P., Mocquet, B. and Cobbold, P.R., 1991: Experiments on simultaneous  
1546 faulting and folding above a basement wrench fault, Tectonophysics, 188, 133-  
1547 141. 1991.
- 1548  
1549 Riedel, W.: Zur Mechanik geologischer Brucherscheinungen. Centralblatt für  
1550 Mineralogie, Geologie und Paläontologie, 1929B, 354-368, 1929.
- 1551  
1552 Riis, F., Vollset, J. & Sand, M.: Tectonic development of the western margin of the  
1553 Barents Sea and adjacent areas. in: M.T.Halbouty (ed.): Future petroleum  
1554 provinces of the World. American Association of Petroleum Geologists Memoir,  
1555 40, 661-667, 1986.
- 1556  
1557 Roberts, D.G., : Basin inversion in and around the British Isles, in: M.A.Cooper &  
1558 G.D.Williams (eds.): Inversion Tectonics. Geological Society of London Special  
1559 Publication, 44, 131-150, 1989.
- 1560  
1561 Ryseth, A., Augustson, J.H., Charnock, M., Haugsrud, O., Knutsen, S.-M., Midbøe,  
1562 P.S., Opsal, J.G. and Sundsbø, G.: Cenozoic stratigraphy and evolution of the  
1563 Sørvestsnaget Basin, southwestern Barents Sea. Norwegian Journal of Geology, 83,  
1564 107-130, 2003.
- 1565  
1566 Saunders, A.D., Fitton, J.G., Kerr, A.C., Norry, M.J., and Kent, R.W.: The North Atlantic  
1567 Igneous Province: Geophysical Monograph 100, American Geophysical Union, 45-  
93, 1997.
- 1568  
1569 Scheurs, G.: Experiments on strike-slip faulting and block rotation, Geology,  
22, 567-570, 1990.
- 1570  
1571 Schreurs, G.: Fault development and interaction in distributed strike-slip shear  
1572 zones: an experimental approach. *in*: Storti, F., Holdsworth, R.E. and Salvini, F.  
1573 (eds): Intraplate Strike-slip Deformation Belts, Geological Society of London  
1574 Special Publication, 210, 35-82., 2003.
- 1575  
1576 Schreurs, G., and Colletta, B.. Analogue modelling of faulting in zones of continental  
1577 transpression and transtension. *in*: Holdsworth, R.E., Strachan, R.A., Dewey, J.F.  
1578 (eds.), Continental Transpressional and Transtensional Tectonics, Geological  
1579 Society of London Special Publication, London, 135, 59-79, 1998.
- 1580  
1581 Schreurs, G. and Colletta, B.: Analogue modelling of continental transpression and  
1582 transtension. *in*: Scellart, W.P. & Passchier, C. (eds.): Analogue Modelling of Large-  
1583 scale Tectonic Processes. Journal of the Virtual Explorer, 7, 103-114, 2003.

1584  
1585 Seiler, C., Fletcher, J.M., Quigley, M.C., Gleadow, A.J and Kohn, B.P.: Neogene  
1586 structural evolution of the Sierra San Felipe, Baja California: evidence of proto-gulf  
1587 transtension in the Gulf Extensional Province? *Tectonophysics*, 488(1), 87-109,  
1588 2010.  
1589  
1590 Sibuet, J.C. and Mascle, J.: Plate kinematic implications of Atlantic equatorial  
1591 fracture zone trends. *Journal of Geophysical Research*, 85, 3401-3421, 1978.  
1592 Sims, D., Ferrill, D.A. and Stamatakos, J.A.: Role of a brittle décollement in the  
1593 development of pull-apart basins: experimental results and natural examples.  
1594 *Journal of Structural Geology*, 21, 533-554, 1999.  
1595  
1596 Sokoutis D.: Finite strain effects in experimental mullions. *Journal of Structural*  
1597 *Geology*, 9, 233-249, 1987.  
  
1598 Stearns, D.W., 1978: Faulting and forced folding in the Rocky Mountains Foreland,  
1599 *Geological Society of America Memoir*, 151, 1-38, 1978  
1600  
1601 Sylvester, A.G. (ed); 1985: Wrench Fault Tectonics, Selected papers reprinted from  
1602 the AAPG Bulletin and other geological journals, American Association of  
1603 Petroleum Geologists Reprint Series 28,3 74pp, 1985.  
1604  
1605 Sylvester, A.G.: Strike-slip faults. *Geological Society of America Bulletin*, 100, 1666-  
1606 1703, 1988.  
1607  
1608 Taylor, B., Goodlife, A. and Martinez, F.: Initiation of transform faults at rifted  
1609 continental margins, *Comptes Rendu Geosciences*, 341, 428-438, 2009.  
1610  
1611 Talwani, M. & Eldholm, O.: Evolution of the Norwegian-Greenland Sea. *Geological*  
1612 *Society of America Bulletin*, 88, 969-999, 1977.  
1613  
1614 Tchalenko, J.S: Similarities between shear zones of different magnitudes.  
1615 *Geological Society of America Bulletin*, 81, 1625-1640, 1970  
  
1616 Tron, V. and Brun J-P.: Experiments on oblique rifting in brittle-ductile systems.  
1617 *Tectonophysics*, 188(1/2), 71-84, 1991.  
  
1618 Twiss, R.J. and Moores, E.M.: *Structural Geology*, 2nd Edition, W.H. Freeman & Co.,  
1619 New York, 736pp, 2007.  
1620  
1621 Ueta, K., Tani, K. and Kato, T.: Computerized X-ray tomography analysis of three-  
1622 dimensional fault geometries in basement-induced wrench faulting, *Engineering*  
1623 *Geology*, 56, 197-210, 2000  
1624  
1625 Uliana, M.A., Arteaga, M.E., Legarreta, L., Cerdan, J.J. and Peroni, G.O.: Inversion  
1626 structures and hydrocarbon occurrence in Argentina. *in*: Buchanan, J.G. &  
1627 Buchanan, P.G. (eds.): *Basin Inversion*, Geological Society London Special  
1628 Publication, 88, 211-233, 1995  
1629

- 1630 Vågnes,E.,1997: Uplift at thermo-mechanically coupled ocean-continent  
1631 transforms: modeled at the Senja Fracture Zone, southwestern Barents Sea. Geo-  
1632 Marine Letters, 17, 100-109, 1997.
- 1633 Vågnes, E., Gabrielsen, R.H. and Haremo. P.: Late Cretaceous-Cenozoic intraplate  
1634 contractional deformation at the Norwegian continental shelf: timing, magnitude  
1635 and regional implications. Tectonophysics, 300, 29-46, 1998.
- 1636 Weijermars, R. and Schmeling, H.: Scaling of Newtonian and non-Newtonian fluid  
1637 dynamics without inertia for quantitative modelling of rock flow due to gravity  
1638 (including the concept of rheological similarity. Physics of the Earth and Planetary  
1639 Interiors, 43, 316–330, 1986.
- 1640 Wilcox, R.E., Harding, T.P. and Selly,D.R.: Basic wrench tectonics. American  
1641 Association of Petroleum Geologists Bulletin, 57, 74-69, 1973  
1642
- 1643 Williams, G.D., Powell, C.M., and Cooper, M.A.: Geometry and kinematics of  
1644 inversion tectonics. in: M.A.Cooper & G.D.Williams (eds.): Inversion Tectonics.  
1645 Geological Society of London Special Publication, 44, 3-16, 1989.  
1646
- 1647 Willingshofer, E., Sokoutis, D. and Burg, J.-P.: Lithosphere-scale analogue modelling  
1648 of collision zones with a pre-existing weak zone, *in*: Gapais,D., Brun.,J.P.&  
1649 Cobbold,P.R. (eds.): DeformationMechanisms, Rhology and Tectonics: from  
1650 Minerals to the Lithosphere, Geological Society London Special Publication,43,  
1651 277-294, 2005.  
1652
- 1653 Willingshofer, E., Sokoutis, D., Beekman ,F. Schönebeck, F., Warsitzka, J.-M.,  
1654 Michael, M. and Rosenau, M.: Ring shear test data of feldspar sand and quartz sand  
1655 used in the Tectonic Laboratory (TecLab) at Utrecht University for experimental  
1656 Earth Science applications. V. 1. GFZ Data Service.  
1657 <https://doi.org/10.5880/fidgeo.2018.072>, 2018.  
1658
- 1659 Woodcock, N.H. and Fisher, M.,1986: Strike-slip duplexes. Journal of Structural  
1660 Geology, 8(7), 725-735, 1986.  
1661
- 1662 Woodcock, N.H. and Schubert, C.: Continental strike-slip tectonics. in: P.L.Hancock  
1663 (ed.): Continental Deformation (Pergamon Press), 251-263, 1994.  
1664
- 1665 Yamada, Y. and McClay, K.R.: Analog modeling of inversion thrust structures,  
1666 experiments of 3D inversion structures above listric fault systems, in: McClay,K.R.  
1667 (ed.): Thrust Tectonics and Petroleum Systems, American Association of  
1668 Petroleum Geologists Memoir, 82, 276-302, 2004.  
1669  
1670  
1671